# TESTING THE USE OF OSL ON COBBLES FROM THE RAISED BEACHES OF KING GEORGE ISLAND, ANTARCTICA

By

PROCOPIOS KOUREMENOS

Bachelor of Science in Geology

University of Alberta

Edmonton, Canada

1999

Submitted to the Faculty of the
Graduate College of the
Oklahoma State University
in partial fulfillment of
the requirements for
the Degree of
MASTER OF SCIENCE
December, 2008

TESTING THE USE OF OSL ON

COBBLES FROM THE RAISED BEACHES

OF KING GEORGE ISLAND, ANTARCTICA

Thesis Approved:

Dr. A. Simms

Thesis Adviser

Dr. R. DeWitt

Dr. J. Puckette

Dr. A. Gordon Emslie

Dean of the Graduate College

ACKNOWLEDGMENTS

Funding for this research was provided by the National Science Foundation, Office of Polar Programs grant #OPP0724929 to Dr. Alexander Simms and Dr. Regina DeWitt Research Cruise NBP-07-03.

TABLE OF CONTENTS

Chapter Page

LIST OF TABLES

LIST OF FIGURES

Figure Page

# CHAPTER I

# INTRODUCTION

## ***A. Introduction***

Reconstructions of the Antarctic Peninsula Ice Sheet (APIS) at the Last Glacial Maximum (LGM) remain poorly constrained due to a lack of geologic data. This scarcity of data has resulted in a variety of ice-sheet models for the APIS during the Late Pleistocene and Holocene (Payne et al. 1989; Nakada et al. 2000; Ivins and James 2005; Bassett et al. 2007). Advances in mapping of the Antarctic shelf have resulted in new constraints on the aerial extent of glaciation at the LGM (e.g. Heroy and Anderson, 2005). However, little data exists for constraining the thickness, volume and melt history of this ice sheet. Sea-level data can be used to estimate the past thickness and volume of ice sheets by comparison with geophysical models of the response of the Earth to ice and water loading (Lambeck, 1993). However, the few sea-level curves that do exist along the Antarctic Peninsula are taken from areas of known tectonic activity or are limited by the use of radiocarbon dating. Radiocarbon dating is limited by the availability of organic material, the poorly constrained radiocarbon reservoir for Antarctica, and the possibility of reworking. Optically Stimulated Luminescence (OSL) is a proven method for obtaining ages from deposits that can not be dated using radiocarbon analysis. Traditionally OSL is used on grains of quartz and feldspar derived from sand. Applying

OSL dating to sediment derived from rocks is in its infancy. The purpose of this study is to test the use of OSL on dating the underside of cobbles within raised beaches in the Antarctic Peninsula. Using OSL dating to obtain ages from cobbles collected from raised beaches along the Antarctic Peninsula will allow for the creation of new sea-level curves for the area. These new sea-level curves will provide important information on the Antarctic Peninsula Ice Sheet thickness and retreat over the Holocene and Late Pleistocene. The hypothesis of this thesis is that OSL ages obtained from minerals derived from the underside of cobbles from the South Shetland Islands will agree with published radiocarbon ages corrected for the appropriate radiocarbon reservoir.

***B. Study Area***

Antarctica is the highest, driest, coldest, and windiest place on earth (USAP 2006). An ice sheet covers the majority of the continent with a maximum thickness of 4776m (USAP 2006). Together with its sea ice, Antarctica influences the heat budget of the earth, deep-sea circulation and sea level (Denton et al. 1991). The entire Antarctic Ice Sheet covers an area of $13.6 \times 10^6$ km$^2$ (Anderson 1999; Denton et al. 1991). The Transantarctic Mountains divide the ice sheet into West and East Antarctica. The study area of this thesis is located at the northern tip of the Antarctic Peninsula, approximately 1000 km south of Tierra del Fuego in South America and separated from South America by the Drake Passage (Figure 1). My study area was the raised beaches that surround Maxwell Bay within King George Island of the South Shetland Islands (Figures 2 and 3). The South Shetland Islands are located 160 km northwest of the Antarctic Peninsula in a

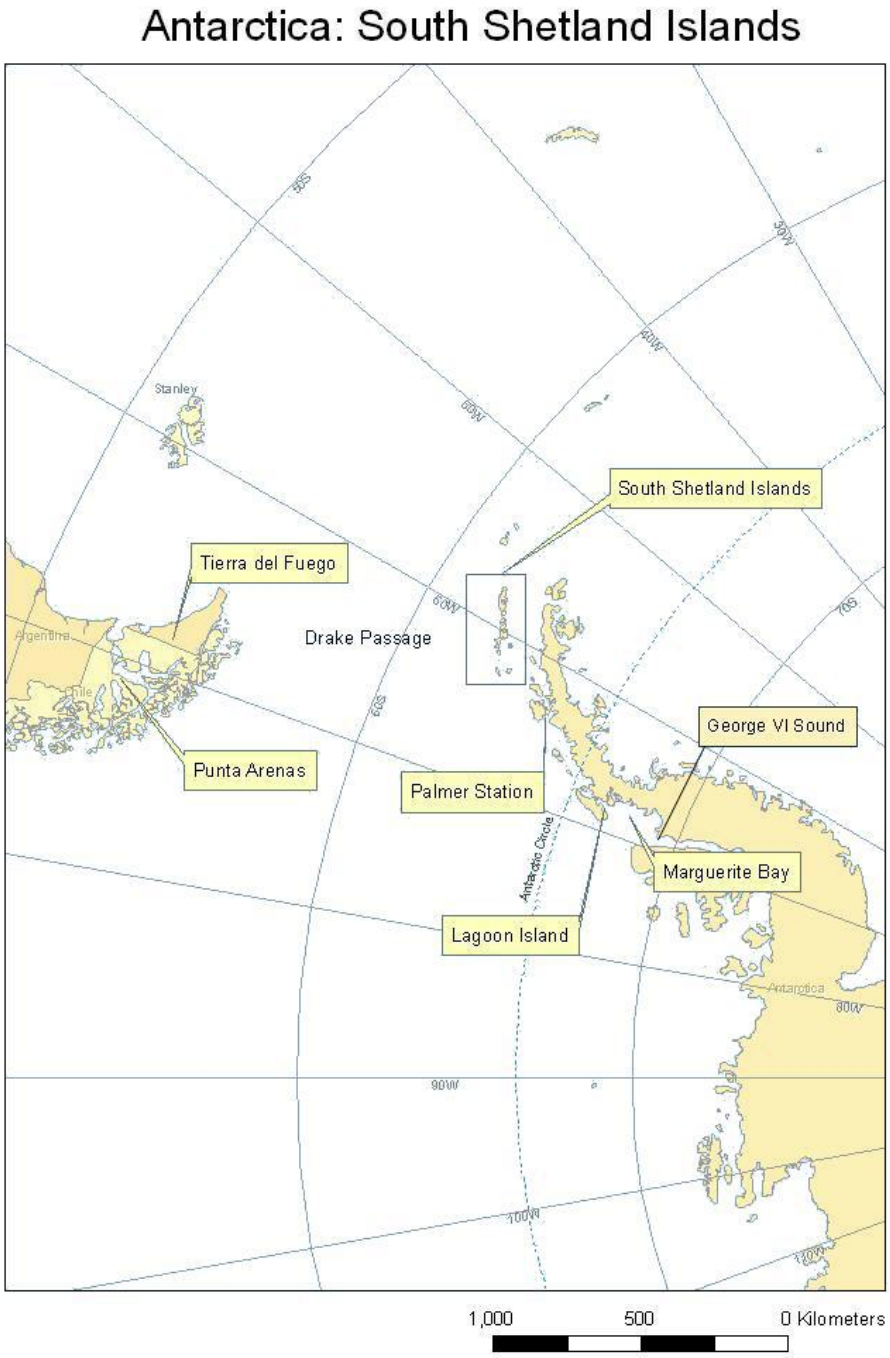


**Figure 1. Location of the South Shetland Islands and the Western Antarctic Peninsula.**

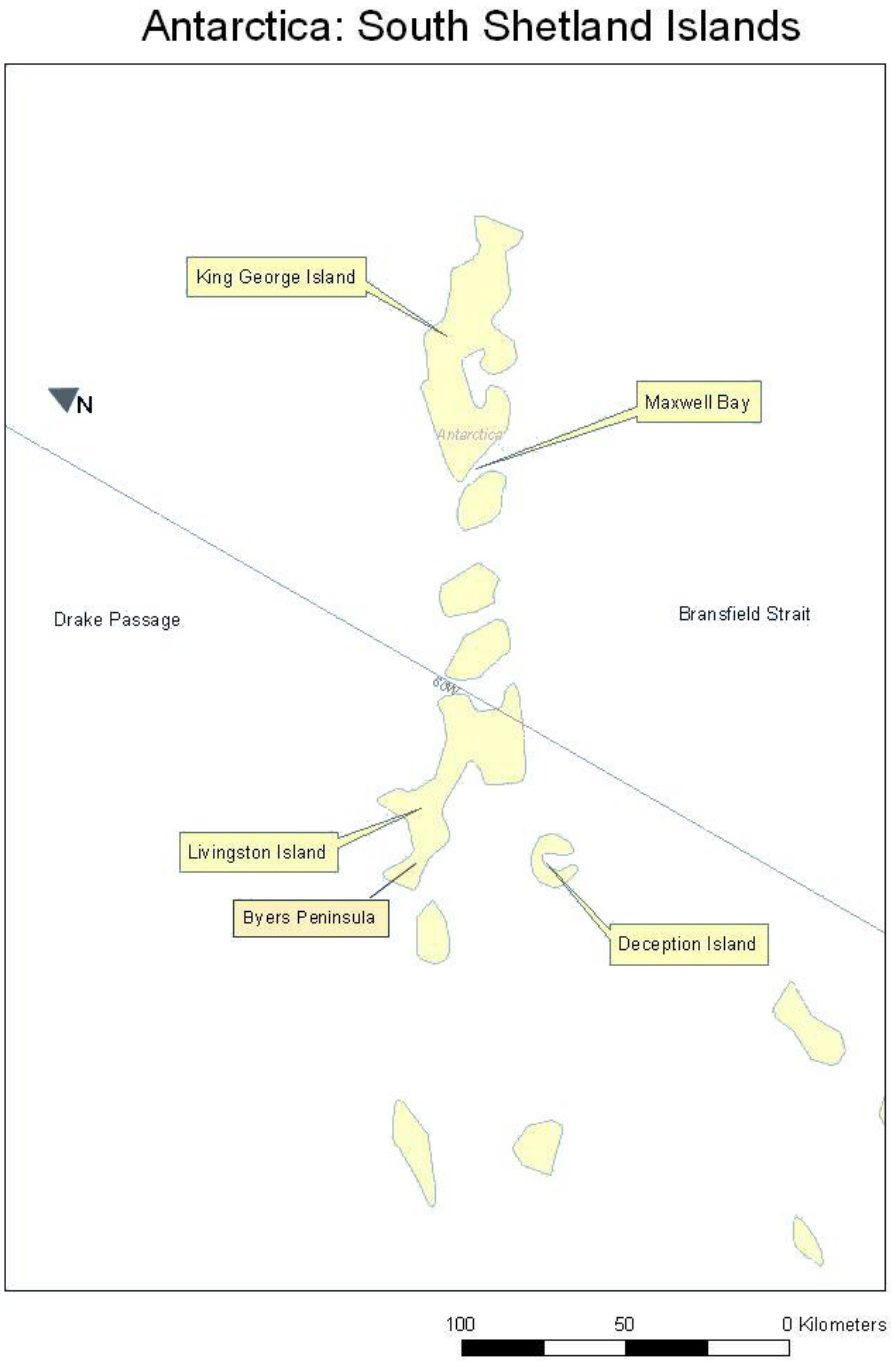


**Figure 2. The South Shetland Islands.**

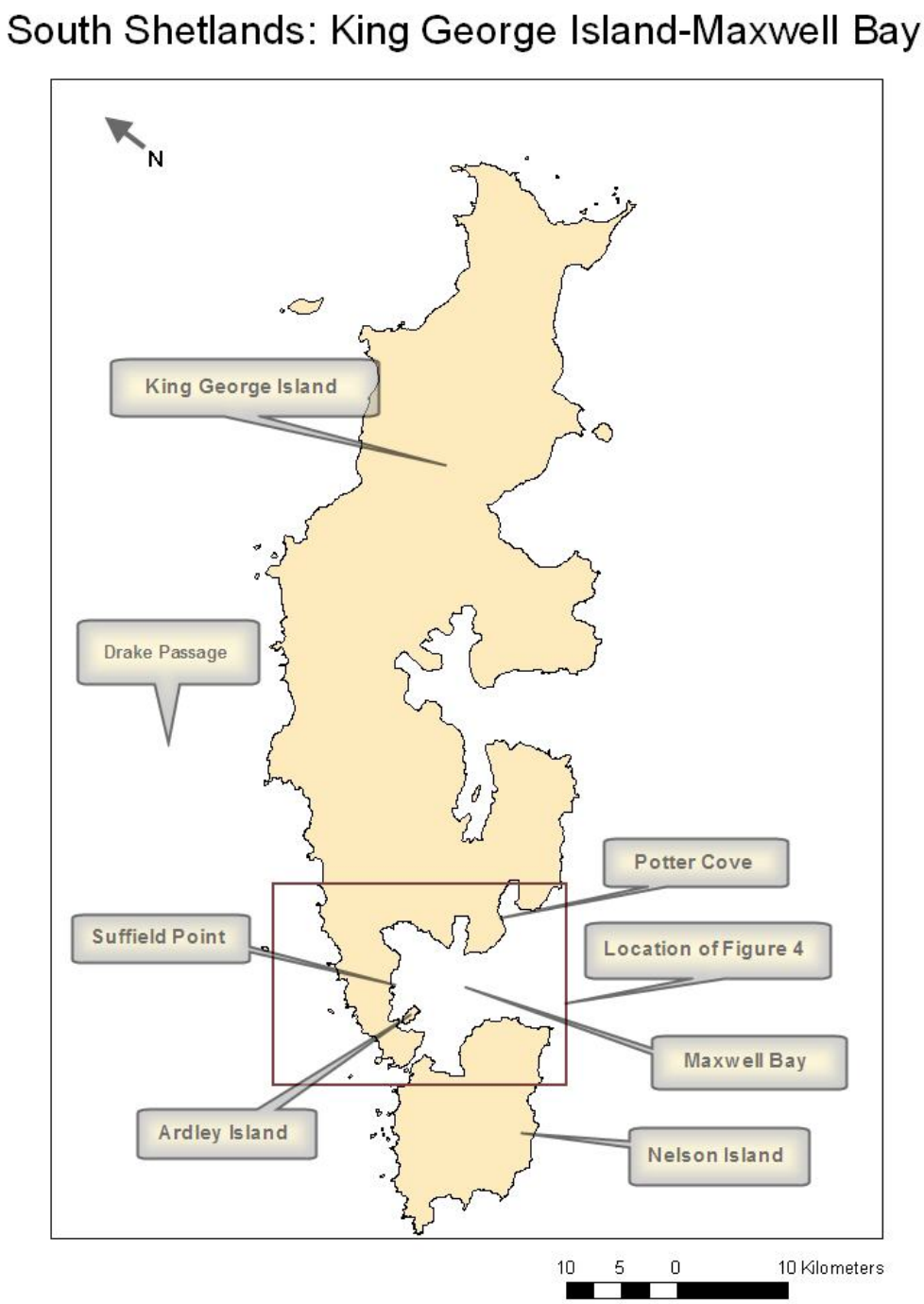


**Figure 3. King George Island of the South Shetland Islands.**

line roughly parallel to the coast of the Antarctic Peninsula (Figure 1). My sample sites include Potter Cove, Suffield Point, and Ardley Island (Figure 4).

### ***C. Climate***

The Antarctic Peninsula lies in a transitional region between polar and sub polar climates. The average temperature of the northern peninsula is slightly above $0^{o}$C in the austral summer and approximately -$12^{o}$C in the winter (Reynolds, 1981). The mean annual isotherm of -$3^{o}$C covers the area through the Bransfield Straight (Yoon et al. 2002). Large amounts of precipitation are recorded on the west-side of the Peninsula. Most precipitation results from cyclonic storms generated in the southern Pacific Ocean. The most intense zone of storm activity and intensity lies around $50^{o}$ S (Anderson, 1999). A zone of low pressure, known as the Antarctic Circumpolar Trough, lies between $65^{o}$S and $70^{o}$S. Winds are highly variable and cyclonic around this area (Anderson, 1999). These winds create rough seas, which can be a potential problem for sampling. The westerly winds of the trough display a bimodal effect, which is strongest in the austral spring and autumn. The temperatures in autumn over the ocean stay warmer longer than those over the continent, due to the temperature lag from the thermal inertia of the ocean (Anderson 1999).

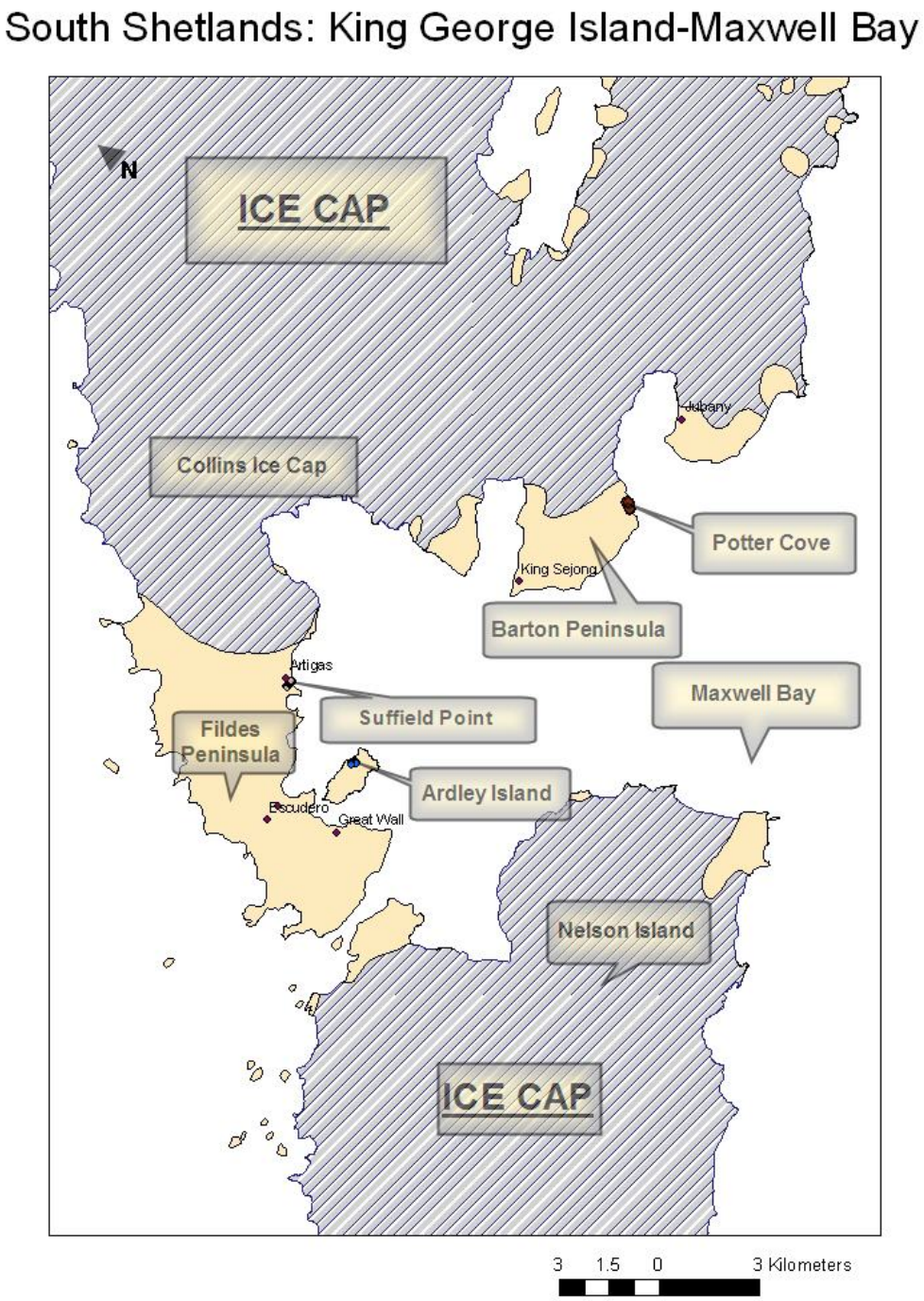


**Figure 4. Maxwell Bay Area showing sampling locations.**

***D. Ice Sheet History***

Change in global climate during the late Cenozoic, particularly in the Southern hemisphere, is impacted largely by the role of the Antarctic Ice Sheet (Shevenell and Kennett, 2007). Eustacy and deep water currents are affected by the presence and or absence of ice. The expansion and contraction of the ice sheet has been recorded in the marine sedimentary record. Global ice volume changes can be measured by eustatic sea-level changes (Lambeck et al., 2002a). Relative sea-level changes must be scrutinized to distinguish between glacial-eustatic effects and local tectonics. It is assumed that changes in sea level of a few tens of meters can be caused by either ice-sheet volume variation or large-scale tectonic events such as an increase in the volume of ocean ridges (Fairbridge, 1961). A major difference between the two is the timing of the events. For glacial-eustatic changes, the magnitude of sea-level fluctuations can be measured in tens of thousands of years; as opposed to tectono-eustatic effects which require millions of years to occur (Vail et al., 1977). The South Shetland Islands are part of an active margin with Deception Island erupting three times in the past 35 years (Barker et al. 1991). Therefore, background rates of tectonic uplift must be taken into consideration when using sea-level data to calculate isostatic rebound for this area.

The ice-sheet history of Antarctica is important because of its potential meltwater contribution to the oceans since the LGM. Denton and Hughes (2002) suggest during the LGM the additional volume of the Antarctic Peninsula sector of Antarctica was 11.55 x $10^5$ $km^3$ out of a total 55.92 x $10^5$ $km^3$ for the entire Antarctic Ice Sheet. This volume of meltwater is approximately 20% of the entire Antarctic meltwater contribution to global sea-level rise over the last 20,000 years. Marine geological and geophysical

investigations such as the sampling of till and the mapping and seismic profiling of megascale glacial lineations, drumlins, moraines, grooves, and flutes provides evidence that the ice sheet on the Antarctic Peninsula was grounded at the shelf edge (Evans et al., 2005; Heroy and Anderson, 2005). The deglaciation of the Antarctic Peninsula commenced when the grounded ice sheet transitioned to an ice shelf around 11-12,000 $^{14}$C a BP (Evans et al., 2005; Heroy and Anderson, 2005). A large-magnitude rise in sea-level around 14,000 $^{14}$C BP, known as meltwater pulse IA (mwp-IA), consituting 20-25% of the rise in eustatic sea-level since the LGM, correlates well with the timing of deglaciation of the Antarctic Peninsula (Bassett et al. 2007), although the ice within the Antarctic Peninsula cannot account for all of the volume of water released during mwp-IA.

# CHAPTER II

# PREVIOUS WORK

## ***A. Previous Work***

Many studies of the ice-sheet history of Antarctica have been conducted over the last 20 years (Yoon et al. 2002; Nakada et al. 2000; Bentley et al. 2005; Payne et al. 1989; Emslie and McDaniel, 2001). All of these studies used radiocarbon dating for the development of a chronological framework. One major limiting factor in the use of radiocarbon dating of fossils and organic material is the radiocarbon reservoir. This radiocarbon reservoir can result in anomalously old age determinations resulting from the mixing of very old carbon that has circulated from deeper bottom waters or from "dead" carbon released from the melting of glacial ice (Curl 1980) with modern carbon. The apparent ages may range from 200 to 2500 years in excess of their true ages (Curl, 1980). More recently, Berkman et al. (1998) calculated the general pre-bomb marine radiocarbon reservoir to be 1300 years for the waters around Antarctica. While studying paleo-penguin colonies, Emslie and McDaniel (2001) utilized a radiocarbon reservoir of 700 years based on a modern penguin bone with an approximate pre-bomb age of 700 BP.

Payne et al. (1989) created an ice-sheet model for the past 40,000 years for the George VI Sound area (south of Marguerite Bay) on the Antarctic Peninsula (Figure 1)

based on parameters such as changes in sea level and marine basal melting. The radiocarbon reservoir used in their calculations was 750 years. From 32,000 BP to 23,000 BP (radiocarbon pre-bomb date) the ice sheet advanced until it reached the shelf edge (Payne et al., 1989). Ice-sheet retreat began at 14,500 BP with a rapid decline at 10,000 to 6500 BP. Eustatic sea level at the early stages of the ice advance was 60 m below present (Payne et al., 1989). Bentley et al. (2005) infer the timing of deglaciation based on radiocarbon dating of shells and penguin remains in the Marguerite Bay area. The highest wave cut platforms and raised beaches in the region were reported to elevations as high as 41 m above mean sea level. If the relative sea-level curve is extrapolated back in time, deglaciation of inner Marguerite Bay occurred prior to 9000 BP. At 3500-2400 BP, a reduction in sea-ice is thought to have occurred resulting in an increase in wave activity (Bentley et al., 2005). The radiocarbon reservoir correction for the Bentley et al. (2005) study relied on a modern penguin bone dated at 1130+/- 134 yr BP. In their study of Adélie penguins, Emslie and McDaniel (2001) found that the occupation of penguin colonies in the Antarctic Peninsula correlates to warming and cooling events in the past. The first occurrence of Adélie penguins on Lagoon Island immediately north of Marguerite Bay (Figure 1) appears around 6000 BP, indicating a glacial retreat by that time.

***B. Optically Stimulated Luminescence (OSL)***

Samples were dated using optically stimulated luminescence (OSL). The method is capable of dating sediment deposits over the last 500,000 years (Forman, 2000). The theory behind OSL dating rests on the ability of defects within the crystal lattice of

common silicate minerals, such as quartz and feldspar, to act as potential storage sites for electrons and as a source for a luminescence signal (Lian and Roberts, 2006).

While sunlight does not have enough energy to completely remove an electron, alpha, beta, and gamma radiation will ionize an atom, creating a free electron. In nature Uranium (U), Thorium (Th), and Potassium (K) are sources of ionizing radiation. In nature the crystal structure of quartz will not always be perfect. Sometimes an atom of Si or O will not be present or will be replaced by atoms of another element. These crystal defects can attract and trap free electrons (Forman et al., 2000).

Exposure to sunlight can stimulate the electrons inside these traps to a higher energy state and release them. As the electron migrates and recombines with the ion, it returns to the original energy state before ionization. As the electron loses energy it emits luminescence.

Thus, exposure to ionizing radiation (alpha, beta, gamma, and cosmic) establishes the luminescence signal (Duller, 2004). The luminescence signal increases with time (Forman, 2000) and as such is proportional to the total exposure from surrounding radiation. This time-stored signal can be released by exposure to light. Exposing the sediment to sunlight resets the OSL clock. Electrons that have accumulated in light sensitive traps within the crystal lattice are measured, providing an age of burial. Dose is proportional to the number of trapped electrons, and thus the luminescence, and describes the energy from the ionizing radiation that is absorbed by the mineral. Equivalent Dose (ED) is the amount of dose administered in the laboratory that creates the same luminescence intensity as the amount of Dose absorbed in nature (Forman, 2000). The ED is determined in the laboratory. Dose Rate is a measure of the rate of

natural radiation levels that induce electron charge transfer, which is measured as luminescence (Greilich et al., 2005). Therefore, to determine an age, equation (1) is used.

$$\text{Age} = \text{Dose}/\text{Dose Rate} \qquad (1)$$

Where Dose is measured in units of Gray which is equal to J/kg; and Dose Rate is measured in units of Gray/annum.

OSL dating has been applied to rock and soil from geoarchaeological sites in Greece, Sweden and a farm in Denmark (Vafiadou et al., 2007). The OSL ages provide information on the last occupation of these prehistoric settlements. Greilich et al. (2005) have used OSL dating on a medieval granitic castle wall in Lindenfels Germany and rocks from geoglyphs in Peru to obtain a date of construction of these structures.

# CHAPTER III

# METHODOLOGY

## ***A. Fieldwork***

We rely on optically stimulated luminescence (OSL) for obtaining ages of sea-level indices. It is therefore important to understand the methodology in order to develop an optimum sampling technique. An important constraint during OSL sampling in the field is that the samples cannot be exposed to blue and green visible light prior to measurement in the laboratory. Consequently, the samples must not be exposed to any light source (e.g. sunlight, UV light, black light, moon light, star light) and care must be taken for the proper collection of samples. In order to block all sources of light, I used a light protecting tarp during sample collection. The tarp consisted of two pieces of heavy light-protecting material sewn together with the seams sealed to prevent light penetration through the needle holes.

Raised beaches were observed in the Maxwell Bay area of King George Island. Reconnaissance of the coastline was completed from the bridge of the R/V *Nathaniel B. Palmer*. Once a raised beach was located, a zodiac was used to transport the researchers from the ship to the beach in order to obtain cobble samples for later optically stimulated luminescence (OSL) analysis. Samples were taken from Potter Cove, Suffield Point, and

Ardley Island (Fig. 4). After landing on the raised beach of interest, the researchers conducted a preliminary investigation of the area and described the sedimentological features of the deposits such as imbrication, grain size and mineralogy. Determining the mineralogy of a sample was difficult due to the snow coverage and the adverse weather conditions encountered. Samples collected were ideally highly felsic due to the necessity of quartz for OSL dating (Forman, 2000).

Cobbles approximately 7 inches by 3 inches were collected. The cobbles sampled were from deposits that either formed a boulder pavement or were well imbricated. In addition, only samples that were well rounded were selected as to ensure that the deposit was part of the paleo-swash zone. Tumbling action within the swash zone would assure that the rock was exposed to sunlight. Once a sample was located, a felt tipped marker pen was used to mark the sample name and indicate the upper surface of the cobble. The heavy light-proof tarp was used to cover the area so the deposits could be sampled. Two scientists worked under the tarp with a rock hammer and chisel to extract the frozen rock. The researchers ensured that no light entered the space beneath the tarp with the exception of a red filtered flashlight, as red light does not damage the OSL sample. They ensured this by holding down the edges of the tarp with their hands/knees/feet and sometimes other rocks. They waited for their eyes to adjust, approximately 60 seconds, to see if any visible light entered the tarp. Once the cobble had been appropriately marked, the tools were used to extract the cobble. Once the rock was extracted it was wrapped in black plastic, and placed in three light-proof black plastic bags. The tarp was then removed and the sample bags labeled and placed in a backpack for transport back to

the ship. Samples of the surrounding rocks, directly adjacent to the OSL sample, would be labeled and placed in clear plastic bags for gamma spectrometry.

***B.GPS***

The precise location and elevation of the sample locations was determined using a Geographical Positioning System (GPS) unit on loan from UNAVCO. The GPS unit consisted of two parts: a base station and a rover unit. The base station consisted of a Trimble R7 powered by a battery and attached with antenna cables to a Zephyr Geodetic disk mounted on a tripod. The rover unit consisted of a Trimble 5700 powered by a battery and attached with an antenna cable to another Zephy disk, which was connected to an attachment pole on the top of a backpack. Both the base station and rover unit had Flash cards (512MB and 256MB respectively) that recorded information and could easily be transferred to a laptop computer. The base station was installed on a 2 m antenna away from any obstacles (seals, penguins) and above the high-water mark. The ideal GPS signal would consist of 6 or more satellites. Once the signal was established the rover unit could be assembled. The rover unit was carried in a backpack and stored the position of multiple waypoints collected during the survey. The height of the Zephy antenna for the rover unit was 1.52 m. If the number of satellite signals fell below the operating number, the unit would be considered "floating". To return to operating mode, it was necessary to wait for satellite signals to be re-established. At each point measured it was necessary to pause in one spot for approximately 15 seconds until a beep was heard from the Trimble 5700 rover unit indicating the information was recorded. Surveys started at contemporaneous sea level. From the point at sea level, the survey commenced

in a straight line climbing the different beach ridges until reaching the highest ridge. Each point and each ridge was recorded in a field book and on the GPS flash card.

Once back aboard the ship, the GPS data from the day was transferred to a laptop computer using Trimble Office software. The base and rover units recorded information in .dat files. The raw data, as well as the field observations of the researcher, were used to estimate the elevations of the beach ridges. For example point number one would be at sea level, although the unit would read 23 m above sea level; thus that point would be adjusted to 0 m.

***i. GPS Processing***

Once back at Oklahoma State University, the unprocessed GPS data was post-processed. To determine the location of the base station, Precise Point Positioning (PPP) was used. The .dat file was converted to a RINEX (Receiver Independent Exchange) file using the Convert to RINEX program in Trimble Office. The .dat file was selected, and then the output file was chosen. The next step was the configuration of the antenna type, which required selecting the "correct to base" and entering the header information (name, number, run). Editing the antenna number required the selection of the bottom of the antenna mount and entering the vertical distance between the bottom of the antenna mount and the survey mark. The survey mark is the point in space whose coordinates will provide the original antenna height. The file was then converted to RINEX.

Once the file was converted it was sent to the Canadian Spatial Reference System. This was done online at http://www.geod.nrcan.gc.ca/online_data_e.php where an account was established. A username and password was provided after the account was

initiated. Using the username and password at http://fcgis1.geod.nrcan.gc.ca/csrstciEN?page=0 and clicking on the CSRS-Precise Point Positioning (PPP) started the processing. The RINEX file previously created was selected along with the static mode of processing using the NAD-83-CSRS reference system. The results were emailed to the account holder in a pdf file format where the Latitude, Longitude and Height were recorded in Trimble Office for the base station.

Once this information had been entered for the base station, the recalculation of the rover points based on the corrected base station was completed. This was done in Trimble Office by clicking on the adjust option under the adjustment menu. To get a corrected elevation, a geoid model, as opposed to the ellipsoid model, was selected from the menu. The geoid model is a more realistic model of the shape of the Earth based on observed gravitational measurements. The projection and datum were changed by clicking on the properties tab in Trimble office. Next, the coordinate system was changed to UTM Zone 20S (find the correct zone referring to http://www.warnercnr.colostate.edu/class_info/nr502/lg3/datums_coordinates/utm.html) and a datum of WGS-84 was selected. The datum is a set of points that act as a latitude and longitude reference. The last step was selecting a geoid model. The EGM96 model, a recommended model for Antarctica, was used (Marianne Okal, UNAVCO, personal communication). After the processing, a general overview of the data was conducted to ensure that the new elevations fit field observations taking into account the tidal range. After processing, the data was exported into ArcMap to create maps of the locations of the raised beaches.

### *ii. Sample Elevations*

Samples were taken from different areas and their elevations were calculated using the GPS surveys. Two sets of elevations are presented, one from GPS elevations corrected to field observations and the other from the post-processed geoid model elevations standardized to WGS-84. The observed elevations were calculated in the following manner. The first point of elevation was taken at the current level of the sea surface. This was interpreted by the scientist in the field to be 0 m with respect to sea level. The raw data from the GPS unit was processed aboard the R/V *Nathaniel B. Palmer* and compared to the field notes. The proper adjustment was made to point 1 of the preliminary-processed data to assign the first point to sea level at the time of measurement. All other measurements were corrected to reflect an elevation of 0 m for the initial point. The results of this method are recorded as the "observed elevations." The "geoid elevations" utilize the GPS data after processing at Oklahoma State University with the aid of UNAVCO and converting the elevations to a geoid model. The samples along with observed and geoid elevations are listed in Table 1.

## *C. OSL*

### *i. OSL Sediment Preparation*

All of our laboratory work for OSL age analysis was conducted in the Radiation Dosimetry Laboratory at Oklahoma State University. A Risø Luminescence Reader was used to determine the Dose. Sample preparation for OSL requires obtaining 90 μm to 212 μm grains of quartz from a large cobble. The procedures must be completed in

**Table 1. Observed and Geoid Elevations.**

| Sample | Location | Observed Elevation (m) | Geoid Elevation (m) |
|---|---|---|---|
| AI-01 | Ardley Island | 11.3 | 9.0 |
| AI-02 | Ardley Island | 11.3 | 9.0 |
| AI-03 | Ardley Island | 11.3 | 9.0 |
| AI-04 | Ardley Island | 6.9 | 4.6 |
| AI-05 | Ardley Island | 7.0 | 4.7 |
| PT-02 | Potter Cove | 8.2 | 5.8 |
| PT-03 | Potter Cove | 8.2 | 5.8 |
| PT-04 | Potter Cove | 8.2 | 5.8 |
| PT-07 | Potter Cove | 0.9 | -1.5 |
| PT-08 | Potter Cove | 0.9 | -1.5 |
| SH-02 | Suffield Point | 9.1 | 7.1 |
| SH-03 | Suffield Point | 9.1 | 7.1 |

darkness (with the exception of red light) to avoid electron stimulation. Our goal was to isolate grains of quartz from the concealed surfaces of the cobbles sampled from the raised beaches and obtain OSL ages from those quartz grains.

***a. Rock Cutting***

The initial stages of sample preparation involve cutting the rock. This was conducted at the HRL (Hazardous Reaction Lab). A windowless room was chosen due to the light sensitivity of the project. A Hillquist 24-inch oil-based saw was used as well as a Hillquist 7-inch water-based saw. Before cutting, the room was darkened and the only permitted light was from a desk light with a red filter (Lee 106, Lee Filters, Inc.). The 24-inch oil-based saw was used to cut the rock, separating the exposed and concealed sides (Figure 5). The rock was placed on the saw in a way to cut along the line drawn by the scientist in the field to indicate the exposed side. The concealed side of the rock was taken and cut into 1-inch cubes using the 7-inch water-based saw.

***b. Slicing***

Bleaching experiments conducted by Dr. Regina DeWitt concluded that sunlight would penetrate up to 5 mm into the rock (DeWitt, personal communication), but the outer 1 mm would most likely be bleached completely. Therefore, for our purposes we cut 1-mm slices from the cubes, i.e. the surface of the rock that was concealed. Enough 1-mm slices were obtained in order to continue the sample preparation. The slicing of the rock occurred in the darkroom of the Radiation Dosimetry Lab of Venture 1. An Isomet 1000 precision saw (Buehler Ltd.) with Isocut Plus cutting fluid was used. Initially the


**Figure 5. Illustration of labeling the top side of a sampled cobble.**

rock was aligned parallel to the blade to ensure a smooth cut. When the rock was in place, the digital scale was zeroed using the dial on the side, and the blade placed to measure 1.5 mm, which after taking into account the thickness of the saw, cut 1-mm thick slices. The slices were collected in the tray of the saw.

***c. Chemical Treatment***

Once the 1-mm slices were cut and collected, the thin slices were crushed using a pestle and mortar to obtain grains that were 90 μm to 212 μm in size. Grains with a defined size range were chosen because beta radiation will not penetrate the entire grain, unlike gamma radiation, which penetrates completely (Aitken, 1999). To calculate the dose rate, corrections had to be applied for the beta attenuation and the correction factors are grain-size dependent. A series of sieves were used to obtain the desired size (90 μm - 150 μm -212 μm). After the grain size was obtained, a series of chemical treatments was used to remove organic material, feldspars, and carbonate (Rittenour et al., 2005; Vafiadou et al., 2007; Schaetzl and Forman, 2008). This chemical treatment consisted of a series of acids starting with 3.7% HCl, then 30% $H_2O_2$, then etching with HF for 40 minutes, and a final rinse of HCl. The chemical treatment with HCl and $H_2O_2$ was done in order to dissolve any carbonates and organics (Vafiadou et al., 2007). The HF etch was done to dissolve feldspar and also to etch the outer portion of the grain to eliminate any effects of alpha radiation (Schaetzl and Forman, 2008). This chemical treatment consisted of a series of acids starting with 3.7% HCl, then 30% $H_2O_2$, then etching with HF for 40 minutes, and a final rinse of HCl. The chemical treatment with HCl and $H_2O_2$ was done in order to dissolve any carbonates and organics (Vafiadou et al., 2007). The HF etch

was done to dissolve feldspar and also to etch the outer portion of the grain to eliminate any effects of alpha radiation (Schaetzl and Forman, 2008). All of the chemical treatment was conducted under a fume hood. Nitrile gloves were used during the chemical treatment. The 90-212 μm grains were transferred from the tray at the bottom of the sieves to plastic 400-ml Nalgene beakers by use of weighing paper. The HCl was added until the grains were submerged. After the reaction was complete, the excess HCl was removed and the grains were rinsed with distilled water. The process of rinsing was repeated three times. The same process was utilized for $H_2O_2$. Next, HF was added and allowed to react for 40 minutes. The fume hood was closed to ensure no toxic fumes escaped. Once 40 minutes elapsed, excess acid was removed and the grains were rinsed. The final step in chemical treatment was an HCl rinse to dissolve fluorite precipitates that might have formed during HF etching. Once again the same steps were taken as previously. The samples were then placed in an oven to dry, awaiting the next step of the sample preparation.

***d. Density Separation***

After the grains were chemically treated, a density separation procedure was used to isolate the quartz (Rittenour et al., 2005; Vafiadou et al., 2007; Schaetzl and Forman, 2008). The density separation method consisted of two steps. The first step isolated heavy minerals, and the second step isolated quartz. A heavy density liquid (Lithium Polytungstate, LST) with a density of 2.85 g/cm$^3$ was used to separate the minerals. Water was added to the LST to change the density to 2.75 g/cm$^3$ in order to isolate the heavy minerals (density > 2.75 g/cm$^3$). Next, more water was added to the LST mixture

until the density of the liquid was 2.62 g/cm$^3$. This liquid was used to separate the quartz from feldspars and any other minerals with density < 2.62 g/cm$^3$. The separation took place in separatory funnels under a fume hood. The chemically treated grains were first placed in the separatory funnels followed by the LST. Separation of the grains occurred after 15 to 30 minutes. While the grains were settling, funnels and filter paper were assembled to catch the grains. The valve on the separatory funnel was opened and the heavy grains were allowed to drain. They were captured in the filter paper. The flask was placed aside and a clean funnel with filter paper was placed under the separatory funnel. The valve was opened and the lighter grains were allowed to drain. The grains were transferred to glass beakers using distilled water. Once in the beaker, the grains were rinsed three times with distilled water to dispose of any excess heavy liquid. After the quartz was collected it was placed in the oven at a temperature of 40°C to dry.

***e. Transfer to Aliquots***

The prepared quartz grains were transferred to 9.7-mm stainless steel aliquots. A silicon spray was used as an adhesive to adhere the grains to the metal aliquots. Approximately 20-50 grains were placed on each aliquot. The aliquots were ready for measurements in the Risø Luminescence Reader.

***ii. OSL Measurements***

***a. Risø Reader***

All measurements were conducted using a Risø TL/OSL reader model TL/OSL-DA-15 (Figure 6). This unit is composed of a light detection system, a luminescence

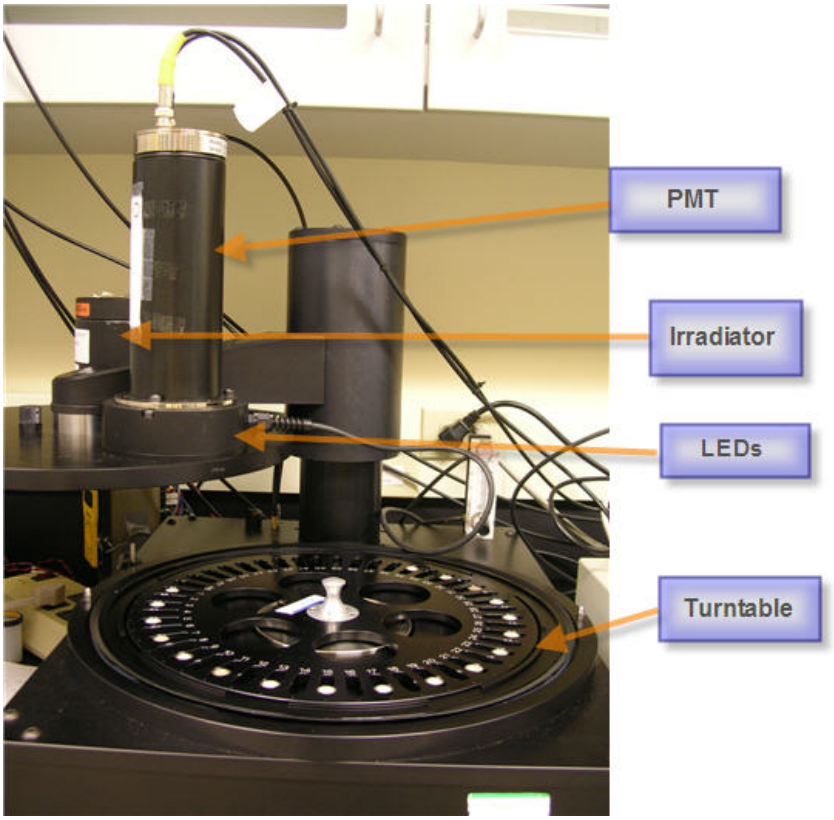


**Figure 6. The Risø reader.**

stimulation system and an irradiation source (Risø Guidebook, 2008). The system program Sequence Editor was utilized to write all sequences and commands to obtain measurements

The aliquots were placed on a sample turntable with 48 slots. The turntable was placed in the sample chamber where the atmosphere was replaced with pure nitrogen. The sample would be lifted through the slots in the turntable to the measurement position by a lift. The stimulation and measurement process could then proceed.

The light detection system consists of a bialkali EMI 9235QB photomultiplier tube (PMT) and suitable detection filters. This PMT has a detection efficiency between 200-600 nm, which is suitable for detection of luminescence of quartz and feldspar (Risø Guidebook, 2008). U340 UV detection filters (Hoya) are used to prevent scattered stimulation light from reaching the PMT and to filter the UV emission of the quartz samples.

An array of blue and infrared (IR) light emitting diodes (LEDs) was used for optical stimulation. The blue (470 nm) LED array sends up to 31 $mW/cm^2$ to the sample and stimulates quartz OSL three times more rapidly than a broad-band light source (Bøtter-Jensen, 2000). A green long pass filter (GG-420) was used in front of the blue diodes to attenuate the blue photons reaching the PMT (Risø Guidebook, 2008). The IR diodes (870 nm) stimulate luminescence in feldspars.

Irradiation was provided by a ($^{90}Sr/^{90}Y$) beta source. The beta source is contained within the irradiator and shielded with lead and aluminum. The source emits beta particles with a maximum energy of 2.27 MeV and a half life of 30 years (Risø Guidebook, 2008). The dose rate is 0.1 Gy/s.

***b. SAR***

To determine the Dose we utilize the Single Aliquot Regenerative (SAR) method (Murray and Wintle, 2000; Wintle and Murray, 2006). This method allows for multiple Dose experiments per single subsample ("aliquot"). In this method a single aliquot undergoes measurement cycles with changing doses. A single-aliquot regeneration sequence for our experiment is shown in Table 2. In the first cycle the natural signal is measured and the first dose was $D_0 = 0$. The following step was a preheat, which was done to remove unstable signals. The preheat temperature needed to be determined individually for each sample and the process is discussed in the following section. The next step was stimulation by blue light. When conducting OSL, the temperature was set to 125°C to increase the stimulation efficiency. The sensitivity of the aliquot can change during the measurement, i.e. even if the aliquot is irradiated with the same dose the resulting luminescence signal can vary. Therefore the sensitivity of the aliquot was monitored by applying a small fixed dose ("test dose") and measuring the resulting luminescence signal. The test dose was applied in step 4 and was approximately 15-20% of the estimated natural dose of the sample. It needed to be determined by a separate dose test. The final step involved stimulating the sample at an elevated temperature. This was done to completely reset the sample.

The regeneration doses ($D_1$, $D_2$, $D_3$, and $D_4$) produced a regenerated OSL dose response which when plotted on a graph is linear (Figure 7). This line was used to correlate the natural signal with the equivalent dose. The doses were chosen in a way that the expected natural dose lays between $D_2$ and $D_3$. The remaining cycles tested the suitability of the measurement procedure for the aliquot under investigation. $D_5$ should

**Table 2. SAR sequence**

| Step | Action | Measurement |
|---|---|---|
| 1 | Beta irradiation with Dose $D_i$ | |
| 2 | Preheat to 210°C for 10s | |
| 3 | OSL at 125°C for 100s | L |
| 4 | Beta irradiation Test Dose | |
| 5 | Preheat to 210°C for 10s | |
| 6 | OSL at 125°C for 100s | T |
| 7 | OSL at 260°C for 40s | |

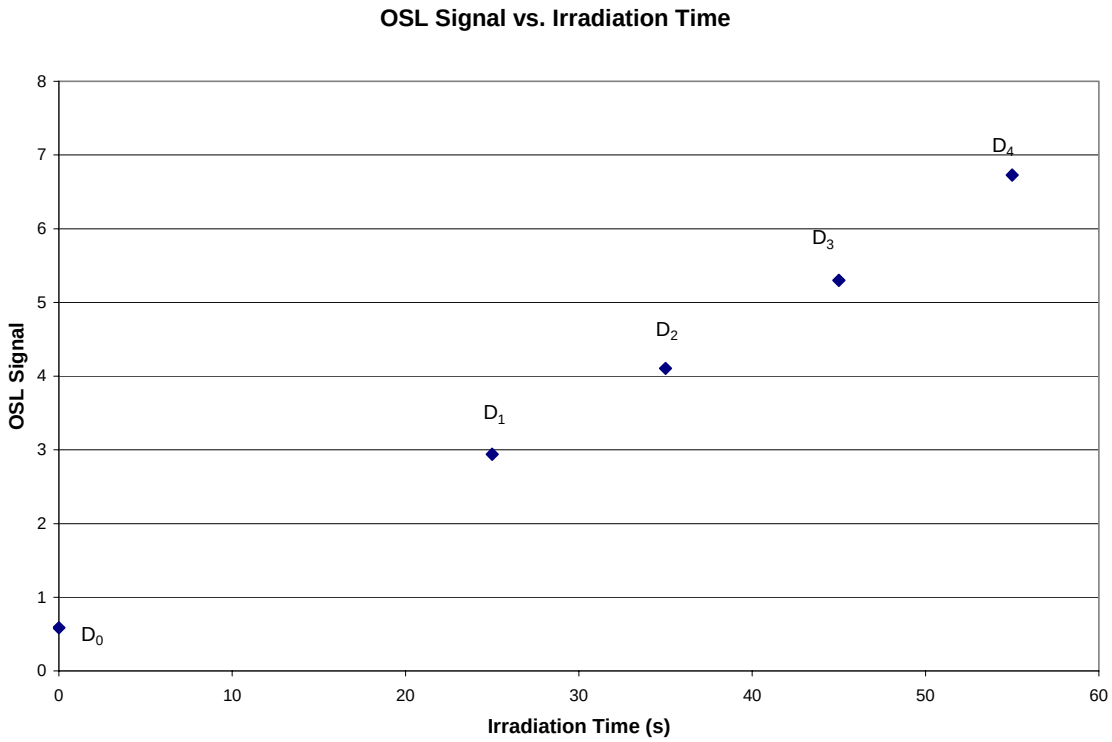


**Figure 7. OSL Signal vs. Irradiation Time ("dose response")**

equal the natural dose, and the dose $D_6$ should equal $D_1$, to show dose recovery. $D_7$ was 0 and this cycle tested if there is an unwanted luminescence signal that does not originate from irradiation. The final dose was $D_8$ which was equal to $D_4$. After $D_8$, Infrared stimulation was conducted to test for feldspar contamination.

***c. Sample Dose and Preheat***

The natural dose of the sample needed to be estimated in order to determine a suitable test dose and regeneration doses. This was completed using 2 aliquots of a sample by first measuring the natural signal of the sample, i.e. the signal resulting from natural radiation. The sample was then irradiated with a known dose and the ratio of the luminescence signals was compared. A sequence was written for the Reader in order for the measurements to be executed by the Reader. The sequence for the sample dose is shown in Table 3.

Once the sample test had been completed, the dose was applied to the sequence used for measurement. For the purpose of our experiment we used the following doses: $D_1$=25, $D_2$=35, $D_3$=45, $D_4$=55, $D_5$=40, $D_6$=25, $D_7$=0, $D_8$=55. These were used for all samples, despite the different natural doses of each sample.

A crystal can hold many different types of defects which result in different traps. "Shallow" traps are not stable over geologic timescales and are empty in the natural state. They are filled, however, during laboratory irradiation and contribute an unwanted OSL signal. Preheating empties these shallow traps. A test was performed to determine the optimum preheat temperature for the OSL measurements. The preheat test required the heating of aliquots of the same sample at various temperatures from 160-300°C for 10s to

**Table 3. Sequence for sample dose.**

| Steps | Sequence |
|---|---|
| 1 | Preheat @ 210°C for 10 seconds and purge with $N_2$. |
| 2 | OSL, blue LED for 100 seconds @ 125°C. |
| 3 | Beta Irradiation for 100 seconds. |
| 4 | Preheat @ 210°C for 10 seconds |
| 5 | OSL, blue LED for 100 seconds @ 125°C. |

determine the variation of the measured Equivalent Dose. Where little variation of the Equivalent Dose with changing preheat temperatures occurs, the points appear to plateau on the graph. The results are shown in Figure 8. The plateau range is from 160-240°C, and 210°C was chosen because it occurs in the middle of our range.

***d. Sequences***

The sequences were created utilizing the Sequence Editor program. A step by step process on how to create a sequence for OSL measurements is listed in Appendix A. Each cycle (steps 1 through 7), must be repeated 9 times for each aliquot to obtain a dose value. There are 7 steps per cycle, and 9 cycles per aliquot. The Risø reader can hold 48 aliquots. In each cycle the dose in step 1 is changed (i.e. $D_1$, $D_2$, $D_3$, $D_4$, $D_5$, etc.). The doses are chosen based on the sample dose test described in Section c.

***e. Data Analysis***

The emitted luminescence is detected by the PMT in the Risø machine and is recorded as photon counts per second. These counts are plotted against time for each measurement (Fig. 9). The signal comprises both luminescence and background signal. As the reading progresses, the luminescence signal decreases and only background signal remains. Therefore the background, (*B)*, must be subtracted from the signal. After the readings were completed in the Risø machine, the results were analyzed using the Analyst Program. This involved taking the integral of the counts measured during the first two seconds (I) of stimulation, and the counts during the last ten seconds divided by

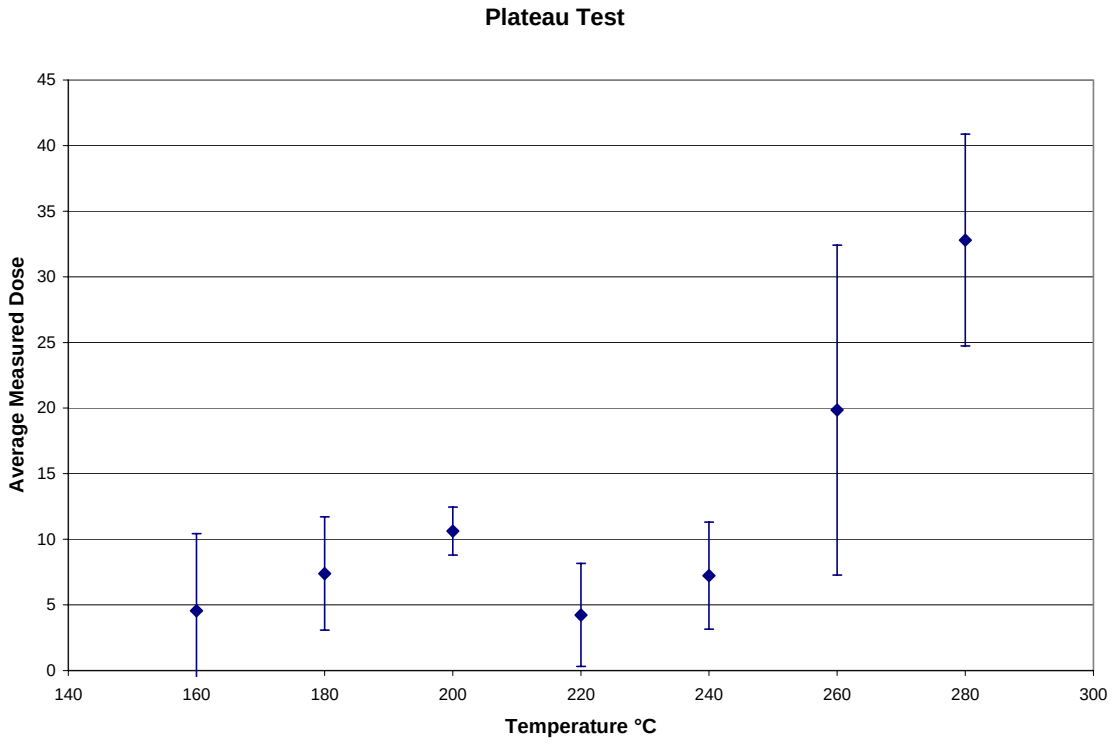


**Figure 8. Preheat plateau test**

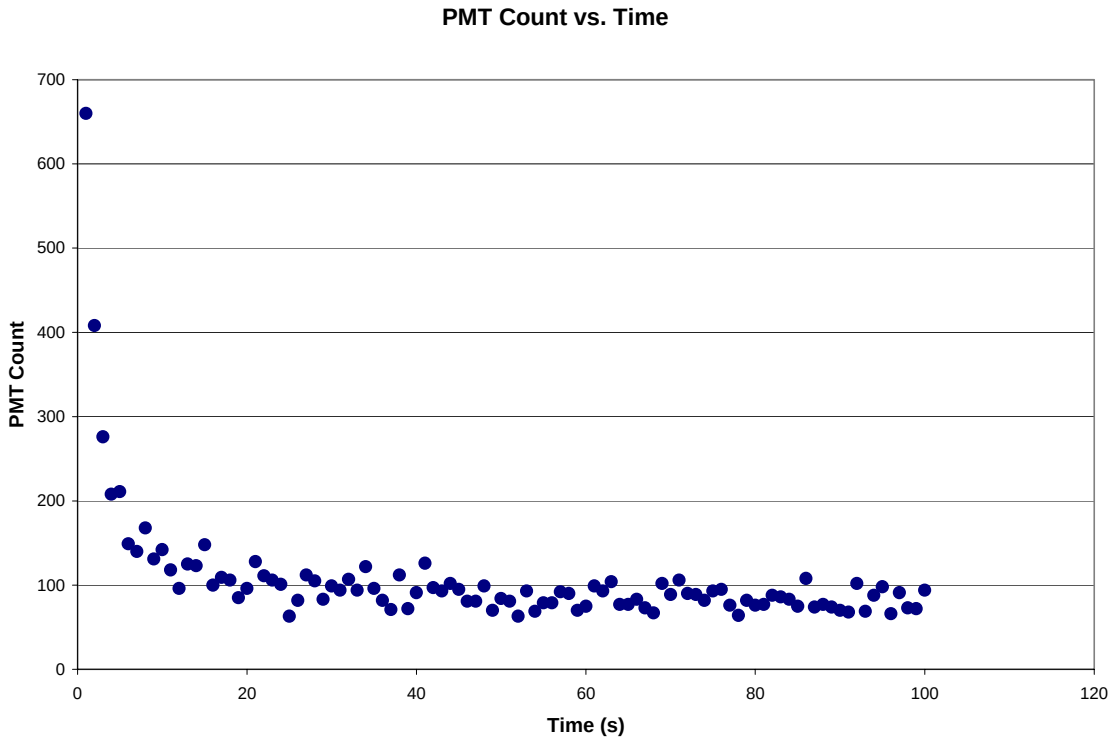


**Figure 9. OSL signal, i.e. PMT Counts measured over time.**

10 (B). The value of L (signal measured after irradiation with dose $D_i$) and T (signal after test dose) is

$$L, T = (I-(2*B)). \quad \text{(Eq. 2)}$$

An error was calculated for both L and T. Next, the sensitivity corrected OSL signal (C) was calculated as

$$C=L/T \quad \text{(Eq. 3)}$$

and an error for C was determined. The C-values corresponding to the doses $D_1$, $D_2$, $D_3$, and D4 were plotted. A linear fit was calculated for this dose response to obtain intercept and slope (*A* and *B*). The equivalent dose corresponding to the natural signal $C_0$ was then calculated using

$$ED = (C_0-A)/B. \quad \text{(Eq. 4)}$$

An error for the Dose was also calculated. Each aliquot had to pass 4 reliability tests (Dose recovery, recycling ratio, recuperation and feldspar contamination). Only aliquots that passed the tests were used for the calculation of the Equivalent Dose, which was calculated as the weighted average of the natural doses obtained with all "good" aliquots. The Equivalent Dose (Gy) of each sample was used to calculate the age using a linear fit.

***iii. Dose rate***

Ionizing radiation stems from radioactive nuclides and cosmic radiation. Gamma radiation has a range of 30-40 cm. Each mineral is exposed to radiation from the surrounding material within this range. In order to determine the amount of background radioactivity, samples were taken from the area surrounding each OSL rock sample. Potassium, uranium, thorium, and their daughter isotopes were measured with gamma

spectrometry. A hammer and jaw crusher were used to smash the rocks down to a smaller size. If the sample was too large, the samples were cut using a 7-inch water-based Hillquist saw. The samples were then broken down to smaller pieces in the jaw crusher. Final grinding occurred at the residency of Dr. Art Lucas utilizing a rock grinder enabling us to obtain the appropriate grain size for measurements. The ground rock was placed in Marinelli containers, weighed, sealed with tape and labeled. Radon gas, which is a daughter of uranium and thorium, escapes during the crushing process. To allow radon and its daughter nuclides time to build up again, the samples are stored for a minimum of three weeks before the measurement. Since the minerals are also affected by the radiation emitted by the OSL sampled rock itself, the material remaining after the slicing process was also crushed, ground down and stored in a separate container. The gamma spectrometry was conducted by Dr. Art Lucas at Lucas Newman Science and Technologies, Inc., and provided the concentrations of uranium, thorium and potassium in the OSL sampled rocks and their surroundings. The results were used as input to calculate the Dose Rate.

The equation for the Dose Rate (Eq. 5) is given below.

$$\text{Dose Rate} = D_{cosmic} + D_{\alpha} + D_{\beta} + D_{\gamma} \qquad \text{(Eq. 5)},$$

where $D_{cosmic}$ is the dose rate contributed by cosmic rays, $D_{\alpha}$ is the contribution by alpha radiation, $D_{\beta}$ is the contribution by beta radiation and $D_{\gamma}$ is the contribution by gamma radiation (Aitken, 1999).

The cosmic dose rate depends on the longitude, latitude, altitude, burial depth, and density of the sample and is calculated according to Prescott and Stephan (1982). The thickness of the cobble was used for the burial depth and the average density was taken to be the average density of andesite (2.8 g/cm$^3$). The outer shell of the grain affected by alpha radiation was dissolved when the grain was etched with HF. Therefore the alpha dose rate does not have to be included. The effect of beta radiation was calculated by using the uranium, thorium, and potassium concentrations (from the gamma spectroscopy) and multiplying by a conversion factor, and a grain-size attenuation factor. The concentrations were converted into dose rate using the dose-rate conversion factors by Adamiec and Aitken (1998). The grain-size correction used an average grain size of 160 μ and attenuation factors after Mejdahl (1979). The gamma dose rate was calculated in a similar way, but without the attenuation factor. Both the beta and gamma dose rates required a correction for the water content. Water absorbs part of the radiation and reduces the total dose rate. While the water content in the rock itself was considered to be negligible, snow and ice will accumulate in the gaps and pores between the cobbles. The water content was calculated by an estimation that involved calculating the pore volume, the volume of ice or snow in the pore, the density of ice or snow or mix thereof, and the amount of time that ice or snow would occupy the pore space. The results of the water content are given in Table 4.

The cosmic dose as well as the total dose rate with error are given in Table 5. The factor listed in Table 5 is needed to take into account the penetration depth of gamma radiation. Beta radiation penetrates a few millimeters into the rock and it is assumed that

**Table 4 Water Content results**

| Sample | Pore Volume Surrounding sample (%) | Weather Conditions when sample taken | Months of Ice | Volume of Ice in Pore (%) | Density of Ice or snow or mix (g/cm3) | Water Content | Water Content Error |
|---|---|---|---|---|---|---|---|
| **AI-01** | 30-60 | snowing | 7 | 50-70 | 0.8 | 0.094 | 0.043 |
| **AI-02** | 30-60 | snowing | 7 | 50-70 | 0.8 | 0.094 | 0.043 |
| **AI-03** | 30-60 | snowing | 7 | 50-70 | 0.8 | 0.094 | 0.043 |
| **AI-04** | 30-60 | cloudy | 7 | 50-70 | 0.8 | 0.094 | 0.043 |
| **PT-03** | 40-60 | sunny | 7 | 50-70 | 0.8 | 0.094 | 0.043 |
| **PT-04** | 40-60 | sunny | 7 | 50-70 | 0.8 | 0.094 | 0.043 |
| **PT-07** | 30-60 | sunny | 7 | 50-70 | 0.8 | 0.094 | 0.043 |
| **SH-02** | 30-60 | cloudy | 7 | 50-70 | 0.8 | 0.094 | 0.043 |

half of the Beta radiation comes from the rock and half from the surrounding material. Gamma radiation on the other hand, has a penetration depth of 30 to 40 cm, which is larger than the diameter of the sample rocks. Dr. Regina DeWitt calculated a correction factor for the Dose Rate to accommodate the size of our samples. This is listed as the factor in Table 5.

### ***iv. Fading***

Fading tests were conducted by Dr. Regina DeWitt as a result of feldspar contamination in the samples. Feldspar undergoes anomalous fading, representing instability in the luminescence traps and causes significant underestimates in age (Auclair and Huot, 2003). The anomalous fading rate is accounted for by the k-value and this factor is used to obtain a fading-corrected optical age. The results of the fading test are shown in Table 6.

**Table 5. Cosmic Dose and Dose Rate**

| Sample | Cosmic Dose Rate (mGy/a) | Cosmic Error (mGy/a) | Factor | Factor Error | Dose Rate (Gy/a) | Dose Rate Error (Gy/a) |
|---|---|---|---|---|---|---|
| **AI-01** | 0.20 | 0.010 | 0.51 | 0.044 | 0.0016 | 0.000037 |
| **AI-02** | 0.20 | 0.010 | 0.55 | 0.034 | 0.0016 | 0.000034 |
| **AI-03** | 0.20 | 0.010 | 0.48 | 0.028 | 0.0015 | 0.000033 |
| **AI-04** | 0.20 | 0.010 | 0.31 | 0.019 | 0.0029 | 0.000070 |
| **PT-03** | 0.21 | 0.010 | 0.22 | 0.020 | 0.0024 | 0.000056 |
| **PT-04** | 0.20 | 0.010 | 0.30 | 0.022 | 0.0024 | 0.000056 |
| **SH-02** | 0.21 | 0.010 | 0.21 | 0.020 | 0.0025 | 0.000058 |

**Table 6. Fading (k) value**

| Sample | k value |
|---|---|
| **AI-01** | 0.04785 |
| **AI-02** | 0.01535 |
| **AI-03** | 0.03626 |
| **AI-04** | 0.00901 |
| **PT-03** | 0.01309 |
| **PT-04** | 0.02269 |
| **SH-02** | 0.00519 |

# CHAPTER IV

# FINDINGS

## ***A. Beach Transects***

The GPS transects across the beach ridges are shown in Figures 10 and 11. The transects clearly indicate that noticeable steps in the topography are present. These steps are interpreted as raised beaches. The evidence for a beach origin includes observations that these steps in the topography are aligned parallel to the shoreline, contain rounded and imbricated cobbles, and have similar slope angles as modern beaches (Figures 12, 13 and 14). Boulder pavements were also observed on the topographic steps of King George Island. Boulder pavements form in response to wave action against loose intertidal gravel (Araya and Hervé, 1972; Hansom, 1983). These pavements are developed in marine settings with an intertidal slope of less than 3° (Hansom, 1983). These topographic steps were also interpreted as beaches by Curl (1980) and John and Sugden (1971). Figures 4, 15 and 16 show the location of the studied raised beaches.

## ***B. OSL Results***

Initially 12 rocks were examined. All samples were granite, granodiorite or granitoid. An important criterion of the entire OSL process is that the rock contains quartz. After cutting the rocks and processing all 12 samples, only 8 were found to

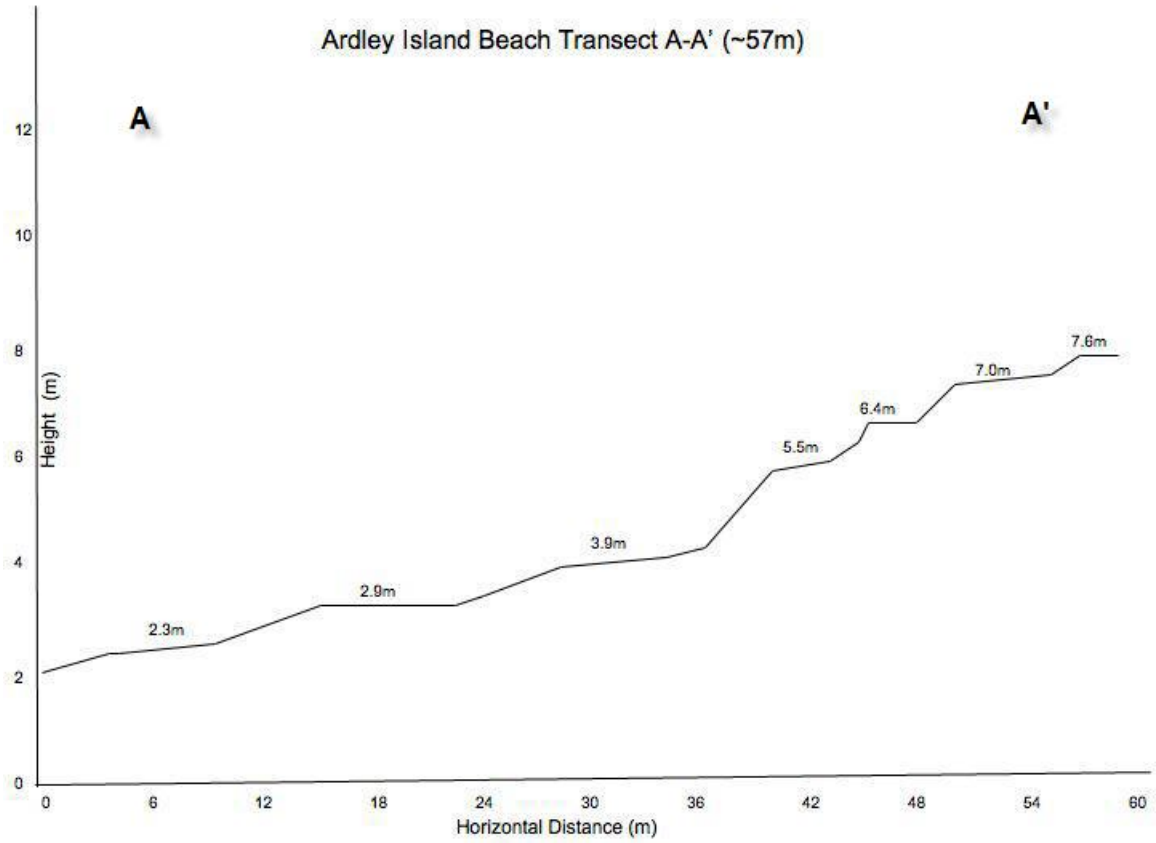


**Figure 10. Ardley Island beach transect. See Figure 15 for transect location.**

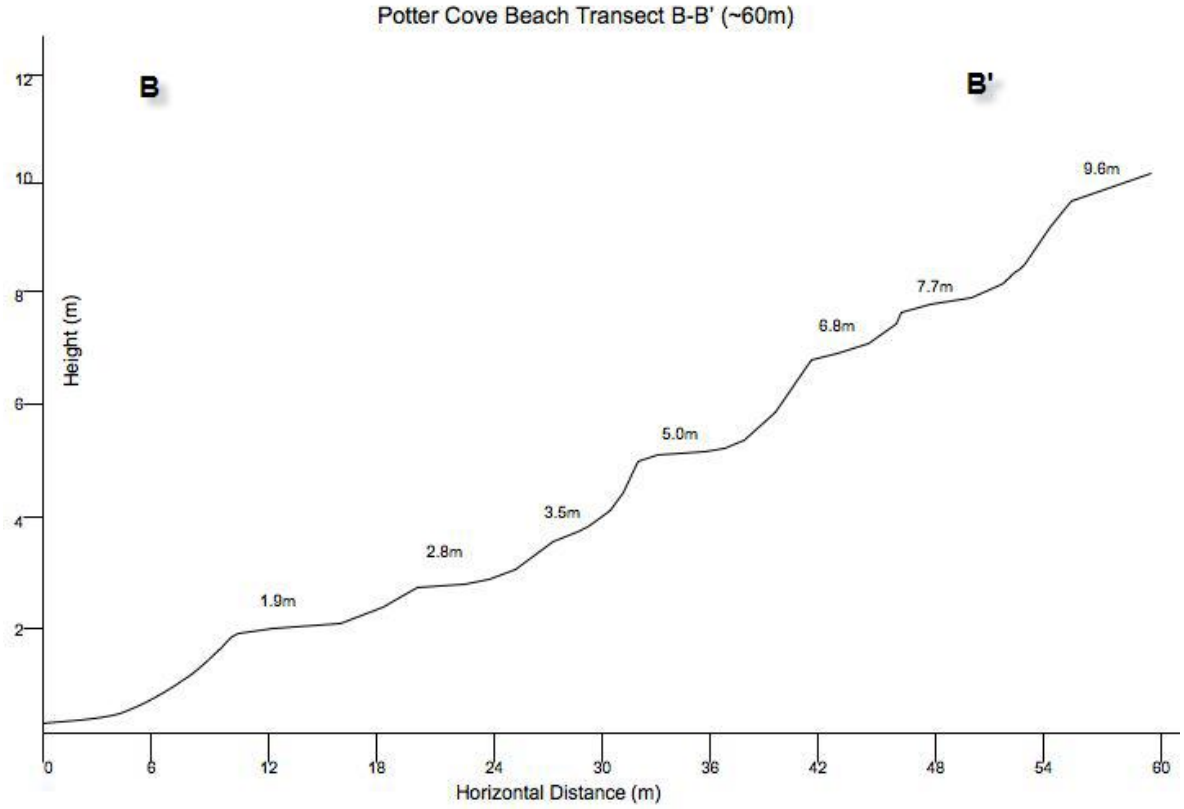


**Figure 11. Potter Cove beach transect. See Figure 16 for transect location.**

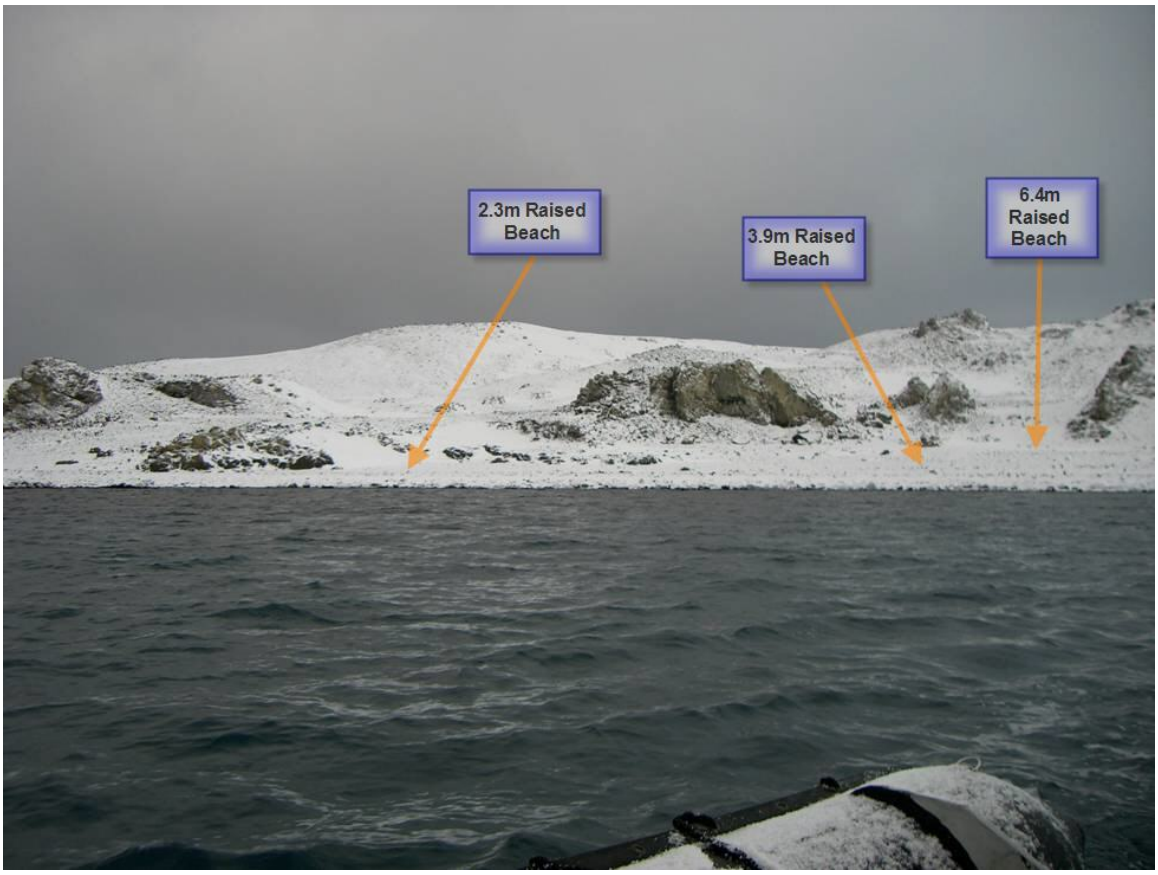

**Figure 12. Raised beaches on Ardley Island.**

**Figure 13. Imbrication of cobbles at a raised beach on Potter Cove.**

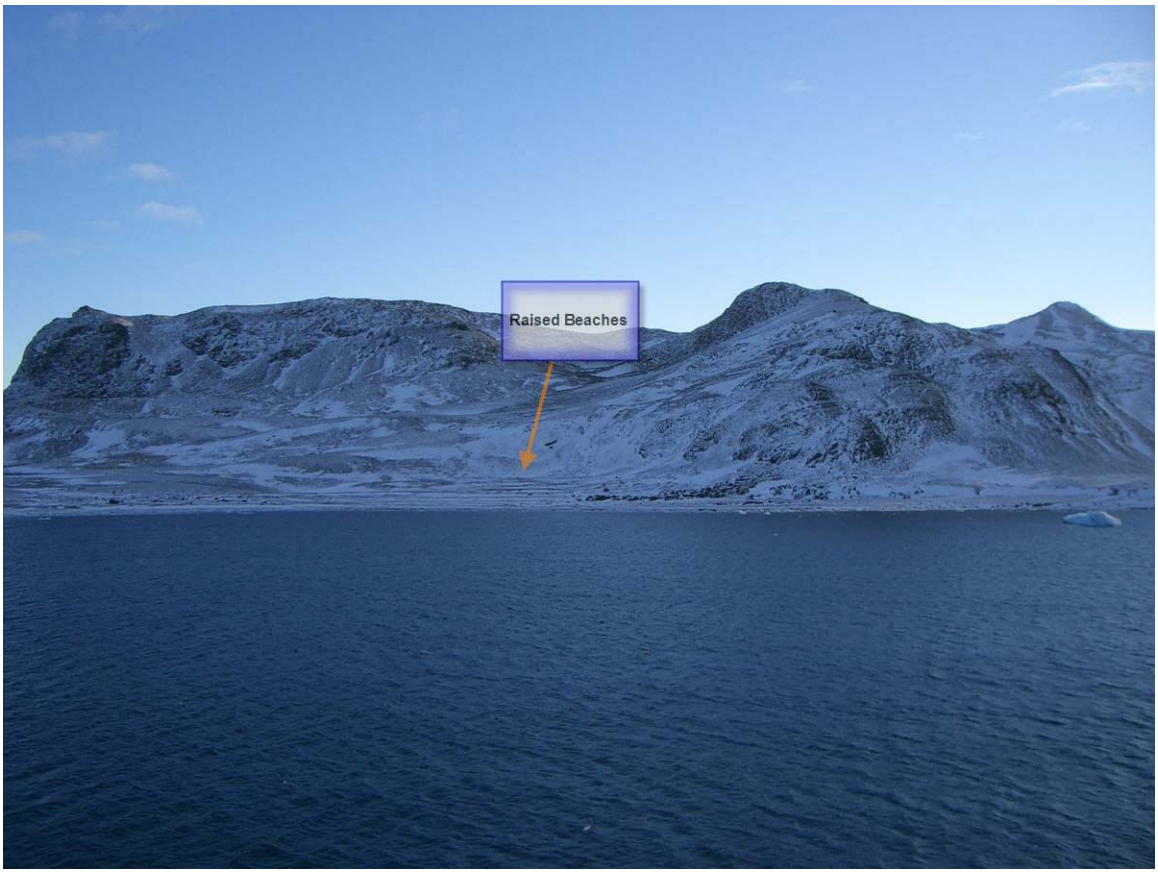


**Figure 14. Raised Beaches at Potter Cove.**

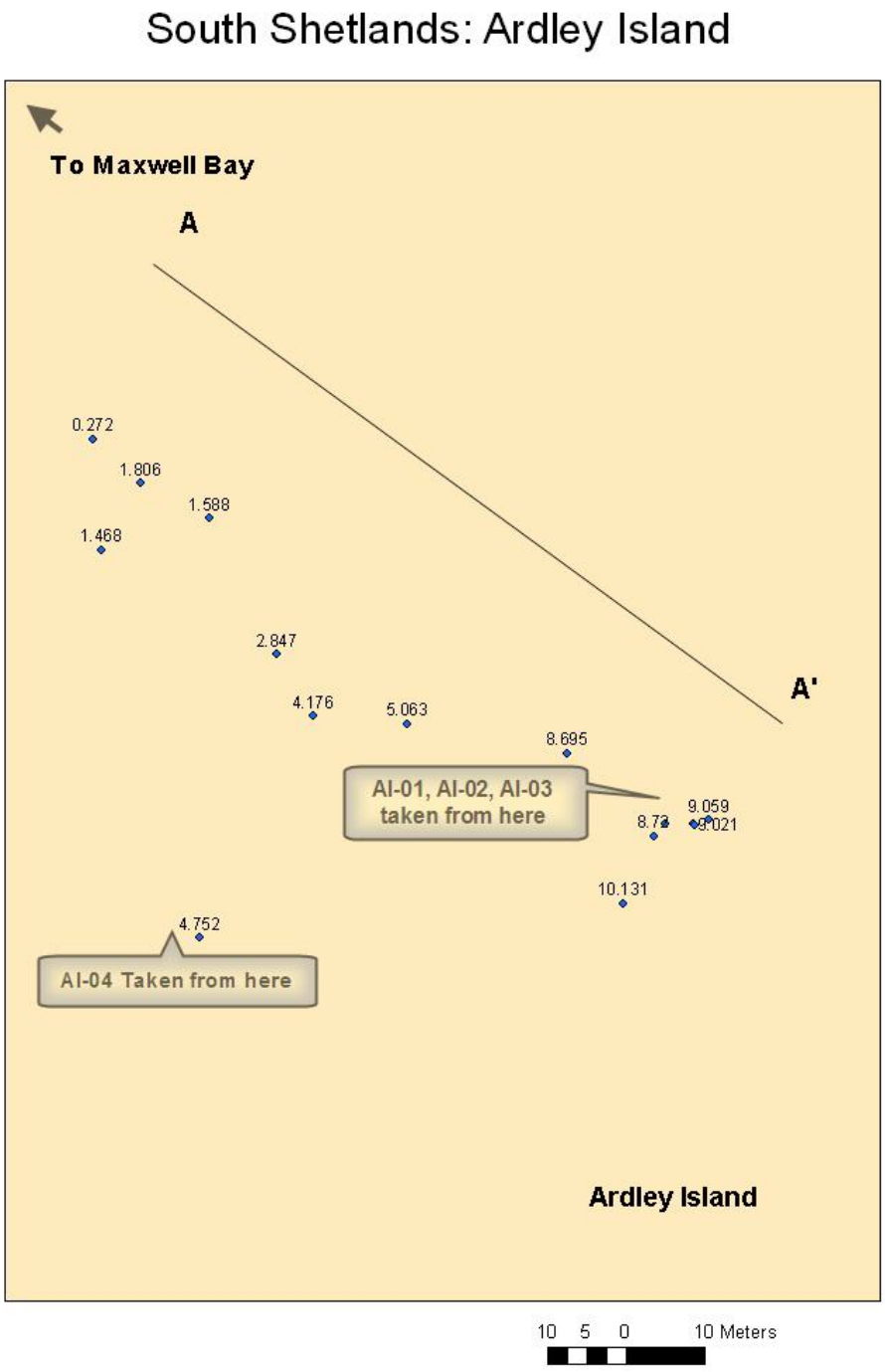


**Figure 15. Ardley Island map with points used to construct elevation transects of the beach ridges (m). Transect taken along A-A'.**

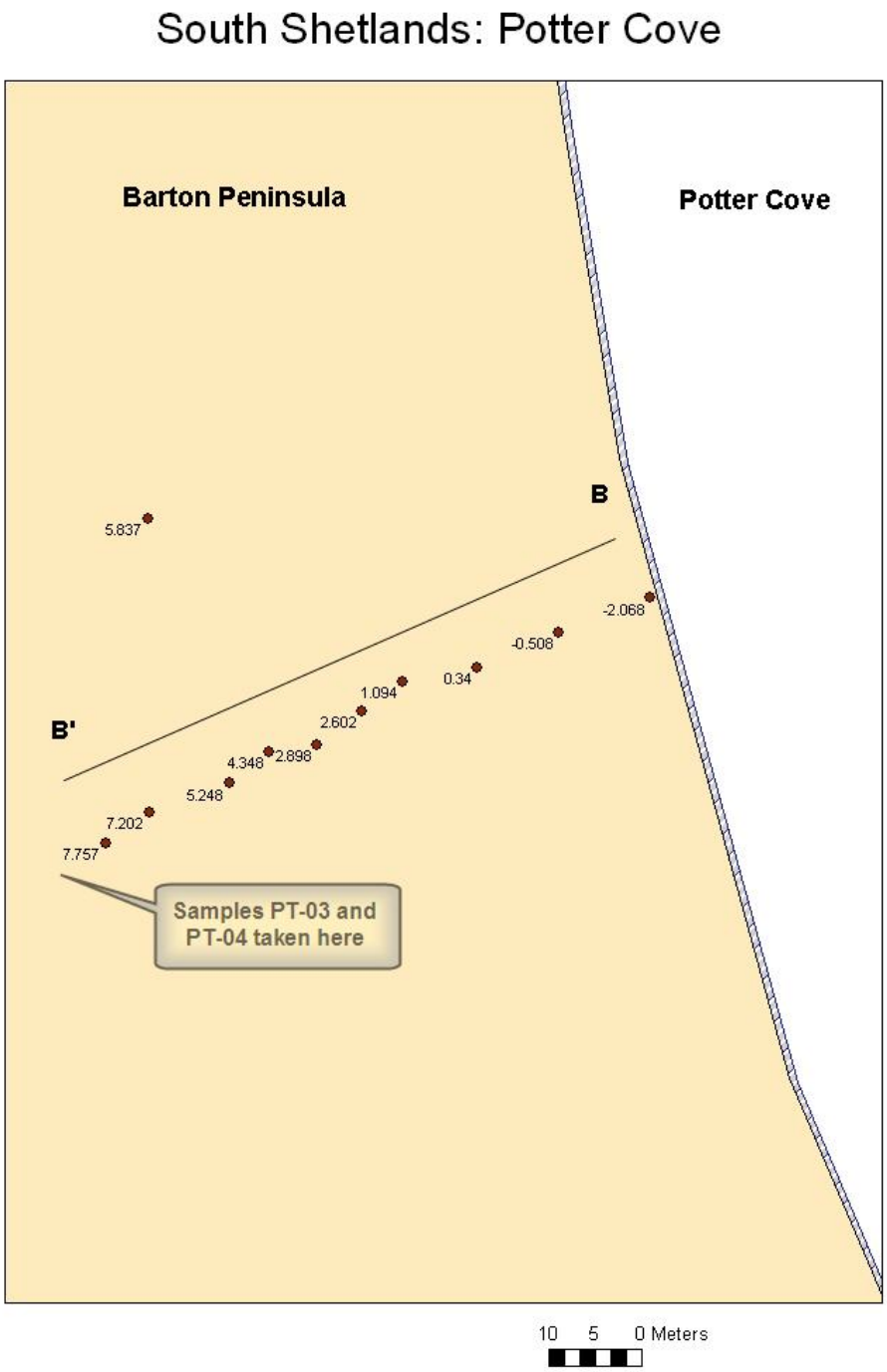


**Figure 16. Potter Cove map with elevations used to construct the transects through the beach ridges (m). Transect taken along B-B'.**

contain enough quartz for OSL measurements (Table 7). The measurements were analyzed and Equivalent Dose and Dose Rate calculated.

Measurements for the samples are summarized in Table 8. The table lists the location of the sample, the observed and geoid elevation, the number of aliquots used for measurements, the Equivalent Dose with error, the Dose Rate with error, and optical age with error. The optical age is calculated from the year the sample was taken; therefore, all ages are calibrated to the year 2007 AD. The optical age for samples AI-01, 02 and 03 from the 9.0-m (geoid elevation) ridge at Ardley Island, are 2048 a +/- 123 a, 1780 a +/- 62 a and 1983 a +/- 198 a, respectively. Sample AI-04 from the ridge at 4.6 m (geoid elevation) has an optical age of 204 a +/- 20 a. Samples PT-03 and PT-04 from Potter Cove show an age of 724 a +/- 261 a and 565 a +/- 96 a, respectively for the ridge at 5.8 m (geoid elevation). The lower ridge within 1.5 m of present sea level (modern beach) at Potter Cove has an optical age of 0. This lower ridge is interpreted as a modern beach ridge as wave heights of up to 1.5 m were observed on modern beaches at Cape Bird during a storm on February 7$^{th}$, 1998 (Butler, 1999). Sample SH-02 taken from a 7.1-m (geoid elevation) ridge at Suffield Point has an optical age of 332 a +/- 332 a. The number of aliquots that were measured reflects the amount of material that was recovered from the sample and suitable for measurements. Sample AI-01, which was a large sample, had 26 aliquots, while SH-02, which was a smaller sample, only yielded 3 "good" aliquots, which is also reflected in the large error.

**Table 7 Sample Type and dimensions**

| Sample | Rock Type | Length (cm) | Width (cm) | Height (cm) |
|---|---|---|---|---|
| AI-01 | Granodiorite | 25 | 20 | 16 |
| AI-02 | Granite | 23 | 21 | 19 |
| AI-03 | Granite | 20 | 17 | 13 |
| AI-04 | Quartzite | 10 | 8 | 7 |
| PT-03 | Granitoid | 10 | 8 | 4 |
| PT-04 | Granite | 12 | 9 | 6 |
| PT-07 | Syenite | 25 | 18 | 12 |
| SH-02 | Diorite | 7 | 7 | 4 |

**Table 8. OSL results**

| Sample | Location | Observed Elevation (m) | Geoid Elevation (m) | Aliquots from sample | Aliquots for age | Equivalent Dose (Gy) | Eq. Dose Error (+/-) (Gy) | Dose Rate (Gy/a) | Dose Rate Error (+/-) (Gy/a) | corrected Optical Age (a) | Optical Age Error (+/-) (a) |
|---|---|---|---|---|---|---|---|---|---|---|---|
| **AI-01** | Ardley Island | 11.3 | 9.0 | 48 | 26 | 1.22 | 0.064 | 1.63 | 0.037 | **2048** | **123** |
| **AI-02** | Ardley Island | 11.3 | 9.0 | 48 | 16 | 1.98 | 0.054 | 1.56 | 0.034 | **1780** | **62** |
| **AI-03** | Ardley Island | 11.3 | 9.0 | 27 | 17 | 0.90 | 0.092 | 1.45 | 0.033 | **1983** | **198** |
| **AI-04** | Ardley Island | 6.9 | 4.6 | 36 | 29 | 0.51 | 0.049 | 2.91 | 0.070 | **204** | **20** |
| **PT-03** | Potter Cove | 8.2 | 5.8 | 18 | 6 | 1.31 | 0.47 | 2.36 | 0.056 | **724** | **261** |
| **PT-04** | Potter Cove | 8.2 | 5.8 | 24 | 15 | 0.82 | 0.137 | 2.42 | 0.056 | **565** | **96** |
| **PT-07** | Potter Cove | 0.9 | -1.5* | 3 | 2 | -0.016 | 0.428 | n/a | n/a | **0** | **0** |
| **SH-02** | Suffield Point | 9.1 | 7.1 | 12 | 3 | 0.75 | 0.784 | 2.48 | 0.058 | **332** | **332** |

* Possible tidal effect

# CHAPTER V

# DISCUSSION

## ***A. Comparison of the dates to each other***

At Ardley Island samples were taken from 2 ridges with different elevations, one ridge at 9.0 m and the other at 4.6 m (geoid elevation). Three samples (AI-01, 02, 03) were taken from the 9.0-m (geoid elevation) ridge and the optical ages were 2048 a +/- 123 a, 1780 a +/- 62 a and 1983 a +/- 198 a. Samples AI-01and AI-03 overlap within the error bars and AI02 is only off by 120 years or 6% of the age. Therefore, the samples show that the 9.0-m (geoid elevation) ridge at Ardley Island is approximately 1900 years old. Two samples were obtained from the 4.6-m (geoid elevation) ridge at Ardley Island, but only one (AI-04), contained quartz. The optical age for AI-04 is 204 a +/- 20 a. The ridge at 4.6 m (geoid elevation) is interpreted to be approximately 200 years old. Comparing the data at Ardley Island shows that the 9.0-m (geoid elevation) ridge is older than the 4.6-m (geoid elevation) ridge. This supports previous work showing that higher beaches are older than lower beaches (Curl, 1980; Bentley et al., 2005).

At Potter Cove, samples were taken from 2 ridges; one at 5.8 m (geoid elevation), and one at -1.5 m (geoid elevation). Samples PT-03 and PT-04 are from the ridge at 5.8 m (geoid elevation). Sample PT-03 has an optical age of 724 a +/- 261 a and sample PT-04 an optical age of 565 a +/- 96 a. These two ages fall within the error bars of one another. The age of PT-04 could be underestimated due to problems with the dose rate

from the sample rock, since it was found underneath sample PT-03. Therefore the 5.8-m (geoid elevation) ridge at Potter cove is interpreted to be approximately 600 years old. Sample PT-07 was obtained from the modern beach at an elevation of -1.5 m (geoid elevation), and the optical age for this sample is 0. This indicates that the rock was completely bleached, consistent with a modern beach in which the cobbles are currently being tumbled, hence resetting the OSL clock. Therefore the 5.8-m ridge is older than the lower ridge at sea level.

Sample SH-02 obtained from a ridge at 7.1 m (geoid elevation) at Suffield Point has an optical age of 332 a +/- 332 a. The optical age error of this sample is very high due to the small amount of quartz isolated. Only enough material for 3 aliquots was obtained. This might have resulted from the small size of the rock and the low quartz content of the rock. Sampling time at Suffield Point was inadequate, which limited the search for quartz bearing rocks. In addition, several of the beach ridges were disturbed by human activity.

***B. Comparison with published dates***

Previously published work by authors including Sugden and John (1973), Hansom (1979), Curl (1980), Mäusbacher et al. (1989), Schmidt et al. (1990), Martinez-Machiavello et al. (1996), Yang and Harwood (1997), del Valle et al. (2002), and Bentley et al. (2005), utilize radiocarbon dating to derive ages for beach ridges in the South Shetland Islands. The purpose of this thesis is to test how well OSL ages agree with radiocarbon ages. Therefore, an age versus height plot of the results of OSL dating from the South Shetland Islands and the calibrated radiocarbon ages after correcting for the

appropriate radiocarbon reservoir as summarized by Bentley et al. (2005), are shown in Figure 17. The OSL ages fit well with the radiocarbon ages. The OSL ages, using the geoid elevations at 5.8 m and 9 m, correlate within error with the Bentley et al. (2005) ridges at 5.5 m, 8 m, and 10 m. The 5.5-m ridge ages reported were collected on Nelson Island and Marion Cove (all within the Maxwell Bay area) and the 8-m and 10-m ridges are located on the Byers Peninsula of Livingston Island.

### ***C. Geological Implications for King George Island***

The beach ridges in this investigation have an age date as well as a measured elevation. A rate of rebound can be calculated by dividing the beach-ridge elevation by OSL age. The rates of rebound were calculated and plotted against distance of the sample site from the Collins Ice Cap (Figure 18). The distance from the ice cap to Suffield Point is 700 m; the distance to Ardley Island is 4000 m; and the distance to Potter Cove is 2000 m. Therefore from the trend on the graph, the rate of rebound decreases with increased distance from the ice cap. This is in agreement with isostatic theory, suggesting that the highest amounts of rebound are found beneath or closest to the former ice caps.

From the data in Figure 17, the rate of rebound has increased over the past 700 years. This is in accordance with the retreat of the Collins Ice Cap at approximately 650 years ago (Hall, 2007). Sampling of moss from two moraines that occur beyond the present ice cap on Fildes Peninsula provide calibrated radiocarbon ages between 654 a

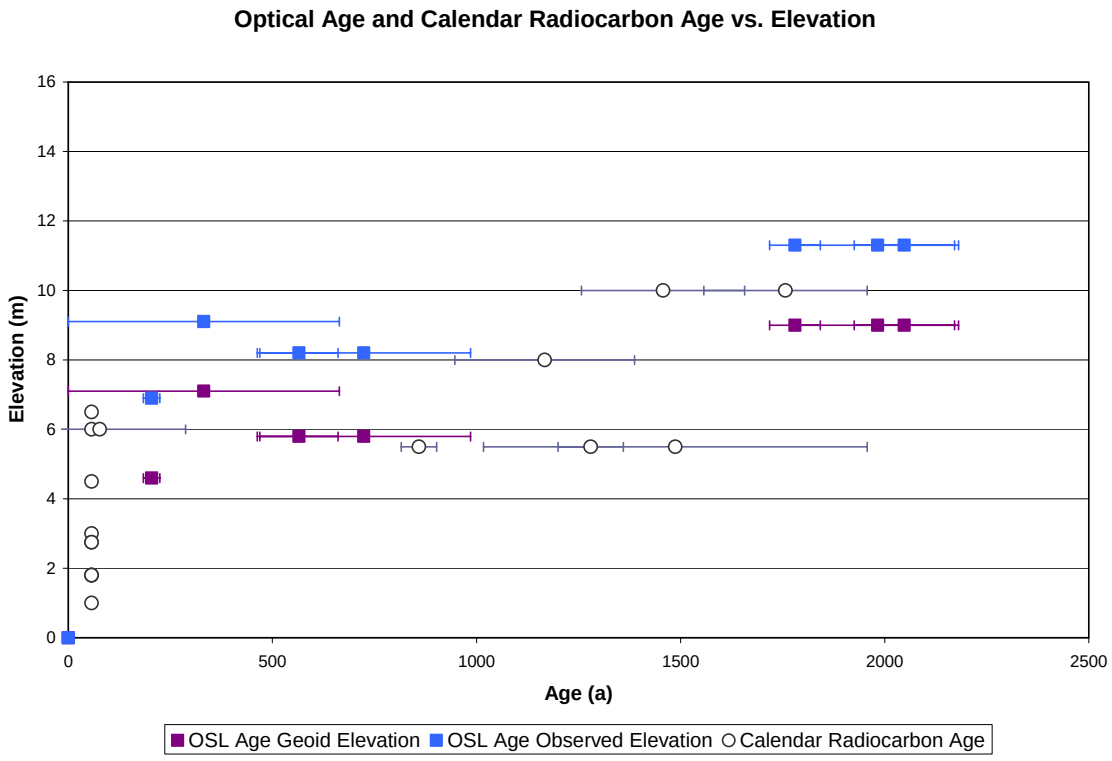


**Figure 17. OSL Age and Radiocarbon Age plotted against elevation. Radiocarbon data from Bentley et al. (2005). See Appendix B for details on the radiocarbon dates.**

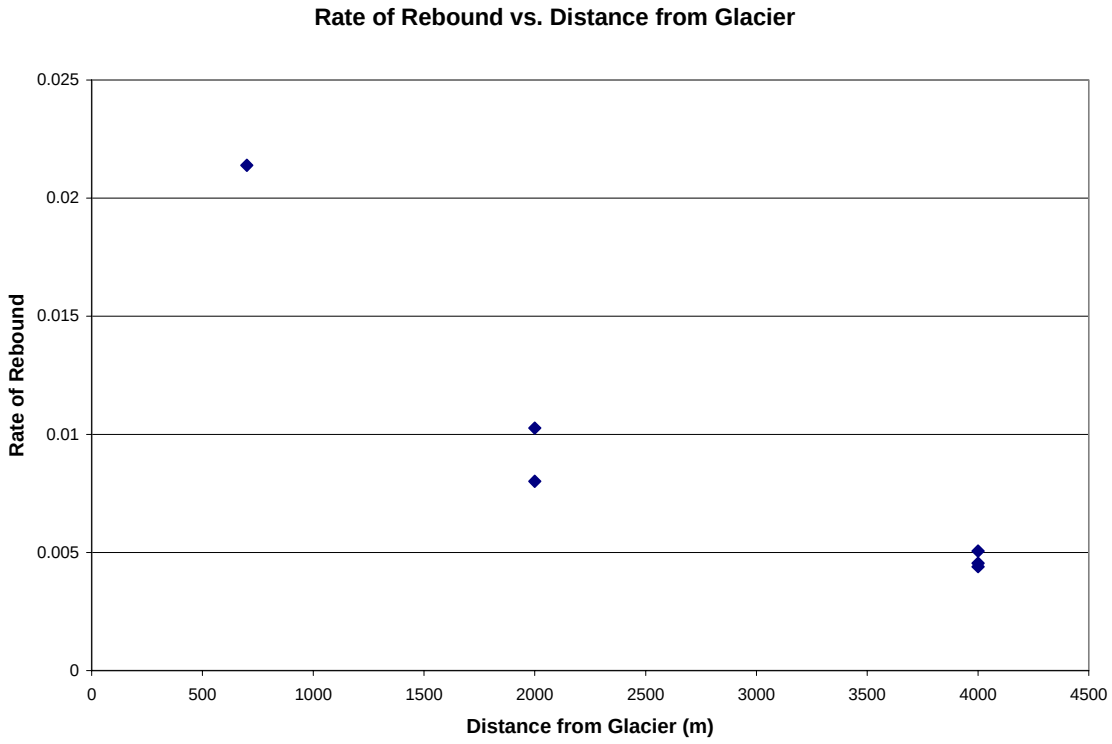


**Figure 18. Rate of rebound compared to distance from glacier.**

+/- 34 a and 1116 a +/- 48 a (Hall, 2007). In order for moss to grow, ice could not have been present suggesting the moraines, which incorporated the moss, are younger than these ages. The glacial advance roughly coincides with the 'Little Ice Age' period (Hall (2007). Hall (2007) suggests the glacier extended ≤400-500 m beyond its current position during this advance.

# CHAPTER VI

# CONCLUSION

## ***A. Conclusion***

The hypothesis of this thesis was that Optically Stimulated Luminescence ages derived from cobbles from raised beach ridges in the South Shetland Islands of the Antarctica Peninsula would compare well with published radiocarbon ages corrected for the carbon reservoir from the same beaches. The application of OSL to material derived from the underside of cobbles in raised beaches of Antarctica is unique. Samples were obtained from raised beaches on Ardley Island, Potter Cove, and Suffield Point in the South Shetland Islands. Elevations for these beach ridges were determined with a GPS survey. Methods were developed to prepare the samples for OSL measurement, as OSL is typically performed on sediment grains, and deriving quartz grains from cobbles is not common practice. The OSL ages correlate very well with published radiocarbon ages. In addition, our ages provide a more precise indication of the timing of an increase in rebound rates on King George Island concurrent with the Little Ice Age. The use of this methodology is not restricted to Antarctica and opens up a myriad of new applications for the use of OSL.

REFERENCES

Adamiec, G., Aitken, M., 1998. Dose-rate conversion factors: update. Ancient TL 16, 2, 37-50.

Aitken, M. J., 1999. Archeological dating using physical phemonena. Rep. Prog. Phys. 62,1333-1376.

Anderson, J.B., 1999. Antarctic Marine Geology. Cambridge University Press, 289pp

Anderson, J.B., Shipp, S.S., Lowe, A.L., Smith Wellner, J., Mosola, A.B., 2002. The Antarctic Ice Sheet during the Last Glacial Maximum and its subsequent retreat history: a review. Quaternary Science Reviews 21, 49-70.

Araya, R., Hervé, F., 1972. Patterned gravel beaches in the South Shetland Islands. Antarctic Geology and Geophysics, Series B, 1, 111-114.

Auclair, M., Huot, M., L., 2003. Measurement of anomalous fading for feldspar IRSL using SAR. Radiation Measurements 37, 487-492.

Barker, P.F., Dalziel, I.W.D., Storey, B.C., 1991. Tectonic development of the Scotia Arc region. In: Tingey, R.J. (Ed.). Geology of Antarctica, Oxford University Press, New York, p. 215-248.

Basset, S.E., Milne, G.A, Bentley, M.J., Huybrechts, P., 2007. Modelling Antarctic sea-level data to explore the possibility of a dominant Antarctic contribution to meltwater pulse IA. Quaternary Science Reviews 26, 17-18, 2113-2127.

Bentley, M.J., Hodgson, D.A., Smith, J.A., Cox, N.J., 2005. Relative sea level curves for the South Shetland Islands and Marguerite Bay, Antarctic Peninsula. Quaternary Science Reviews 24, 1203-1216.

Berkman, P.A., Andrews, J.T., Björck, S., Colhoun, E.A., Emslie, S.D., Goodwin, I.D., Hall, B., Hart, C.P., Hirakawa, K., Igarashi, A., Ingólfsson, O., López-Martínez, J., Lyons, W.B., Mabin, M.C.G., Quilty, P.G., Taviani, M., Yoshida, Y., 1998. Circum-Antarctic coastal environmental shifts during the Late Quaternary reflected by emerged marine deposits. Antarctic Science 10, 3, 345-362.

Bøtter-Jensen, L., Bulur, E., Duller, G.A.T., Murray, A.S., 2000. Advances in luminescence instrument systems. Radiation Measurements 32, 523-528.

Butler, E.R.T., 1999. Process environments on modern and raised beaches in McMurdo Sound, Antarctica. Marine Geology 162, 105-120.

Curl, J.E., 1980. A glacial history of the South Shetland Islands, Antarctica. Ohio State University. Institute of Polar Studies, report No. 63, 129pp.

dell Valle, R.A., Montalti, D., Inbar, M., 2002. Mid-Holocene macrofossil-bearing raised marine beaches at Potter Peninsula, King George Island, South Shetland Islands. Antarctic Science 14, 263-269.

Denton, G.H., Prentice, M.L., Burckle, L.H., 1991. Cainozoic history of the Antarctic ice sheet. In: Tingey, R.J. (Ed.). Geology of Antarctica, Oxford University Press, New York, p. 365-433.

Denton, G. H., Hughes, T.J., 2002. Reconstructing the Antarctic Ice Sheet at the Last Glacial Maximum. Quaternary Science Reviews 21, 193-202.

Duller, G.A.T., 2004. Luminescence dating of Quaternary sediments: recent advances. Journal of Quaternary Science 19, 2, 183-192.

Emslie, S.D., McDaniel, J.D., 2002. Adélie penguin diet and climate change during the middle to late Holocene in northern Marguerite Bay, Antarctic Peninsula. Polar Biol 25, 222-229.

Evans, J., Pudsey, C.J., ÓCofaigh, C., Morris, P., Domack, E., 2005. Late Quaternary glacial history, flow dynamics and sedimentation along the eastern margin of the Antarctic Peninsula Ice Sheet. Quaternary Science Reviews 24, 741-774.

Fairbridge, R.W., 1961. Convergence of evidence on climatic change and ice ages. Annals New York Academy of Sciences, 542-579.

Forman, S.L., Pierson, J., Lepper, K., 2000. Luminescence Geochronology. In: Quaternary Geochronology: Methods and Applications, AGU Reference Shelf 4, p. 157-176.

Greilich, S., Glasmacher, U.A., Wagner, G.A., 2005. Optical dating of granitic stone surfaces. Archaeometry 47, 3, 645-665.

Hall, B., 2007. Late-Holocene advance of the Collins Ice Cap, King George Island, South Shetland Islands. The Holocene 17, 8, 1253-1258.

Hansom, J., 1979. Radiocarbon dating of a raised beach at 10m in the South Shetlands. BAS Bulletin 49, 287-288.

Hansom, J.D., 1983. Ice-formed intertidal boulder pavements in the sub-Antarctic. Journal of Sedimentary Petrology 53, 1, 135-145.

Heroy, D.C., Anderson, J.B., 2005. Ice-sheet extent of the Antarctic Peninsula region during the Last Glacial Maximum (LGM)-Insights from glacial geomorphology. GSA Bulletin, 117, 11/12, 1497-1512.

Ivins, E.R., James, T.S., 2005. Antarctic glacial isostatic adjustment: a new assessment. Antarctic Science 17, 4, 541-553.

John, B.S., Sugden, D.E., 1971. Raised marine features and phases of glaciation in the South Shetland Islands. BAS Bulletin 24, 45-111.

Lambeck, K., 1993. Glacial rebound and sea-level change: an example of a relationship between mantle and surface processes. Tectonophysics, 223, 15-37.

Lambeck, K., Yokoyama, Y., Purcell, T., 2002a. Into and out of the last glacial maximum: sea-level change during oxygen isotope stages 3 and 2. Quaternary Science Reviews 21, 343-360.

Lambeck, K., Esat, T.M., Potter E.K., 2002b. Links between climate and sea levels for the past three million years. Nature, 419, 199-206.

Lian, O.B., Roberts, R.G., 2006. Dating the Quaternary: progress in luminescence dating of sediments. Quaternary Science Reviews 25, 2449-2468.

Martinez-Macchiavello, J.C., Tatur, A., Servant-Vildary, S., del Valle, R., 1996. Holocene environmental change in a marine-estuarine-lacustrine sediment sequence, King George Island, South Shetland Islands. Antarctic Science 8, 313-322.

Mäusbacher, R., Müller, J., Schmidt, R., 1989. Evolution of post-glacial sedimentation in Antarctic lakes (King George Island). Zeitschrift für Geomorphologie 33, 219-234.

Mejdahl, V., 1979. Thermoluminescence dating: beta-dose attenuation in quartz grains. Archaeometry 21, 1, 61-72.

Murray, A.S., Wintle, A.G., 2000. Luminescence dating of quartz using an improved single-aliquot regenerative-dose protocol. Radiation Measurements 32, 57-73.

Nakada, M., Kimura, R., Okuno, J., Moriwaki, K., Miura, H., Maemoku, H., 2000. Late Pleistocene and Holocene melting history of the Antarctic ice sheet derived from sea-level variations. Marine Geology 167, 85-103.

Payne, A.J., Sugden, D.E., Clapperton, C.M., 1989. Modeling the growth and decay of the Antarctic Peninsula ice sheet. Quaternary Research 31, 119-134.

Prescott, J. R., Stephan, L.G., 1982. The contribution of cosmic radiation to the environmental dose for thermoluminescent dating. PACT, 6, 17-25.

Reynolds, J.M., 1981. The distribution of mean annual temperatures in the Antarctic Peninsula. British Antarctic Survey Bulletin 54, 123-133.

Risø DTU, Guide to the Risø TL/OSL Reader, February, 2008. Risø National Laboratory, Roskilde, Denmark.

Rittenour, T.M., Goble, R.J., Blum, M.D., 2005. Development of an OSL chronology for Late Pleistocene channel belts in the lower Mississippi valley, USA. Quaternary Science Reviews 24, 2539-2554.

Schaetzl, R.J., Forman, S.L., 2008. OSL ages on glaciofluvial sediment in northern Lower Michigan constrain expansion of the Laurentide ice sheet. Quaternary Research 70, 81-90.

Schmidt R., Mäusbacher, R., Müller, J., 1990. Holocene diatom flora and stratigraphy from sediment cores of two Antarctic Lakes (King George Island). Journal of Paleolimnology 3, 55-90.

Shevenell, A.E., Kennett, J.P., 2007. Cenozoic Antarctic cryosphere evolution: tales from deep-sea sedimentary records. Deep-Sea Research II, 54, 2308-2324.

Sugden, D.E., John, B., 1973. The ages of glacier fluctuations in the South Shetland Islands, Antarctica. In: Palaeoecology of Africa, the Surrounding Islands and Antarctica. Balkema, cape Town, 141-159.

United States Antarctic Program (USAP), Participant Guide. NSF 06-52. 2006-2008 Edition

Vafiadou, A., Murray, A.S., Liritzis, I., 2007. Optically stimulated luminescence (OSL) dating investigations of rock and underlying soil from three case studies. Journal of Archaeological Science 34, 1659-1669.

Vail, P.R., Mitchum, R.M. Jr., Thompson, S. III, 1977. Seismic stratigraphy and global changes of sea level, part 3: relative changes of sea level from coastal onlap. AAPG Memoir 26, 63-81.

Wintle, A.G., Murray, A.S., 2006. A review of quartz optically stimulated luminescence characteristics and their relevance in single-aliquot regeneration dating protocols. Radiation Measurements 41, 369-391.

Yang, S., Harwood, D.M., 1997. Late Quaternary environmental fluctuations based on diatoms from Yanou Lake, King George Island, Fildes Peninsula, Antarctica. In: The Antarctic Region: Geological Evolution and Processes. Terra Antarctica Publication, Siena, 853-859.

Yoon, H.I., Park, B-K, Kim, Y., Kang, C.Y., 2002. Glaciomarine sedimentation and its paleoclimatic implications on the Antarctic Peninsula shelf over the last 15 000 years. Palaeogeography, Palaeoclimatology, Palaeoecology 185, 235-254.

APPENDICES

Appendix A

***Creating a Sequence***

1) Go to Options-Sequence Options-Run 1 at a time. Set Nitrogen to purge for 10 seconds.
2) Double click under Samples and enter sample set such as #1, 3, 5, 7…etc as this reflects aliquot position.
3) In Run 1 double click and enter 0 or leave blank.
4) In Run 2 , pre-heat: enter temperature of 210°C. Select heating rate of 5°C/s for 10s. At this step we purge nitrogen. Go to the $N_2$ button and click nitrogen flow (start nitrogen flow 10s, end $N_2$ off).
5) In Run 3 click OSL, light source blue LED, time 100s, during stimulation 100, read temperature 125°C. Heating rate 5°C/s.
6) In Run 4 is Beta Irradiation. Here we insert the number from the beta test.
7) In Run 5 we pre-heat enter temperature of 210°C. Select heating rate of 5°C/s for 10s.
8) In Run 6 click OSL, light source blue LED, time 100s, during stimulation 100, read temperature 125°C. Heating rate 5°C/s.
9) In Run 7 click OSL, light source blue LED, time 40s, during stimulation 40, read temperature 260°C. Heating rate 5°C/s.

10) On the last cycle of one sample you insert an Infrared dose. Click OSL, light source IR diodes, time 100s, during stimulation 100, read temperature 60°C.

Appendix B

Radiocarbon data collected from Bentley et al. (2005)

| Laboratory code | Conventional $^{14}$C age (yr BP) | Corrected $^{14}$C age (yr BP) | Alt. amsl (m) | Material Dated | Reference |
|---|---|---|---|---|---|
| Birm-50 | 1056 ± 130 | modern | 3.00 | Whalebone (collagen) | Sugden and John (1973) |
| SRR-1086 | 2823 ± 40 | 1400 ± 200 | 10 | Whalebone (collagen) | Hansom (1979) |
| SRR-1087 | 3121 ± 35 | 1700 ± 200 | 10 | Whalebone (collagen) | Hansom (1979) |
| I-7869 | 1025 ± 80 | modern | 4.50 | Whalebone | Curl (1980) |
| DIC-372 | 840 ± 75 | modern | 1.80 | Whalebone (collagen) | Curl (1980) |
| I-7870 | 2530 ± 85 | 1110 ± 220 | 8 | Whalebone (collagen) | Curl (1980) |
| I-7872 | 4905 ± 100 | 3480 ± 220 | 2 | Whalebone | Curl (1980) |
| DIC-370 | 970 ± 50 | modern | 1.80 | Sealbone | Curl (1980) |
| Birm-224 | 1390 ± 140 | modern | 6.50 | Whalebone (collagen) | Sugden and John (1973) |
| Birm-496 | 674 ± 66 | modern | 1.00 | Whalebone (collagen) | Sugden and John (1973) |
| DIC-367 | 1000 ± 45 | modern | 1.80 | Whalebone (collagen) | Curl (1980) |
| DIC-368 | 1200 ± 110 | modern | 2.75 | Whalebone (collagen) | Curl (1980) |
| DIC-369 | 1210 ± 55 | modern | 2.75 | Whalebone (collagen) | Curl (1980) |
| DIC-371 | 1360 ± 165 | modern | 6.00 | Whalebone (collagen) | Curl (1980) |
| DIC-373 | 1440 ± 55 | 20 ± 210 | 6.00 | Whalebone (collagen) | Curl (1980) |
| Birm-16 | 1223 ± 81 | 1223 ± 80 | 5.50 | Seaweed | Sugden and John (1973) |
| Birm-17 | 1430 ± 470 | 1430 ± 470 | 5.50 | Seaweed | Sugden and John (1973) |
| Birm-14 | 802 ± 43 | 802 ± 43 | 5.50 | Tree Trunk (*Nothofagus Antarctica*) | Sugden and John (1973) |
| Not given | 5750 ± 40 | 4620 ± 140 | 16 | Penguin bone | del Valle et al. (2002) |
| Not given | 5840 ± 40 | 4710 ± 140 | 15 | Penguin bone | del Valle et al. (2002) |

VITA

Procopios Kouremenos

Candidate for the Degree of

Master of Science

Thesis: THE DEGLACIATION OF THE ANTARCTIC PENINSULA USING OSL DATING FROM BEACH DEPOSITS

Major Field: Geology

Biographical:

Personal Data: Born in Edmonton, Alberta, Canada in 1976.

Education: Graduated from the University of Alberta in Edmonton, Canada in 1999 with a Bachelor of Science in Geology. Completed the requirements for the Master of Science in Geology at Oklahoma State University, Stillwater, Oklahoma in December, 2008.

Experience: Currently working in the Geoscience field at Samson Resources in Tulsa, Oklahoma.

Professional Memberships: Member of the American Association of Petroleum Geologists (AAPG), Geological Society of America (GSA), American Geophysical Union (AGU), Tulsa Geological Society (TGS), and Canadian Society of Petroleum Geologists (CSPG)

Name: Procopios Kouremenos Date of Degree: December, 2008

Institution: Oklahoma State University Location: Stillwater, Oklahoma

Title of Study: TESTING THE USE OF OSL ON COBBLES FROM THE RAISED BEACHES OF KING GEORGE ISLAND, ANTARCTICA

Pages in Study: 68 Candidate for the Degree of Master of Science

Major Field: Geology

Scope and Method of Study: The purpose of this thesis is to find a new method for dating raised-beach deposits in order to create more accurate sea-level curves for the Antarctic Peninsula. We test the use of optically stimulated luminescence (OSL) in dating cobbles from raised beaches within the South Shetland Islands of the Antarctic Peninsula. OSL is commonly used for sediment, but the application to rocks is in its infancy. Methods were developed to isolate quartz grains from the cobbles for OSL measurement.

Findings and Conclusions: Of the 12 samples I attempted to obtain age dates from, 8 contained enough material for OSL analysis. The OSL ages are in agreement with calibrated radiocarbon ages from the same deposits. In addition, the OSL ages are all internally consistent in that ages obtained from higher ridges are always older than lower ridges and ages obtained from the same ridges overlap one another. My results also clearly illustrate a change in rebound rates within the South Shetland Islands roughly coincident with recent glacier expansion recorded by the mapping and dating of moraines. Because of the large radiocarbon reservoir in Antarctica, OSL is shown to be a more precise method for dating raised beaches than radiocarbon techniques.

ADVISER'S APPROVAL: Dr. A. Simms